Instrument Familiarization Plan for ground based observations of SPSS. I. CCD Shutter Characterization and Linearity Evaluation

prepared by: G. Altavilla, E. Pancino, S. Marinoni, G. Cocozza, M. Bellazzini, A. Bragaglia, J.M. Carrasco, L. Federici
approved by: F. van Leeuwen & C. Cacciari
reference: GAIA-C5-TN-OABO-GA-004
issue: 1
revision: 0
date: 2011-05-11
status: Issued

Abstract

This document reports the analysis of the minimum shutter time, shutter delay and linearity for the CCDs used in the ground based telescopes devoted to the Gaia absolute calibration programme.

Document History

Issue	Revision	Date	Author	Comment
1	0	11-May-2011	GA	final version
D	5	19-Apr-2011	GA	EP comments added
D	4	28-Mar-2011	GA	CJ, MB, LF comments included
D	3	08-Feb-2011	GA	draft to be circulated
D	2	13-Jan-2011	GA	EP comments
D	1	11-JAN-2010	GA	First version

Acronym	**Description**
ADU	Analogue-to-Digital Unit
BFOSC	Bologna Faint Object Spectrograph & Camera
BUSCA	Bonn University Simultaneous CAmera
CAFOS	Calar Alto Faint Object Spectrograph
CAHA	Centro Astronómico Hispano Alemán
CCD	Charge-Coupled Device
DOLORES	Device Optimized for LOw REsolution Spectroscopy
EFOSC2	ESO Faint Object Spectrograph & Camera
ESO	European Southern Observatory
IRAF	Image Reduction and Analysis Facility (NOAO)
NTT	New Technology Telescope (ESO)
OB	Observing Block
REM	Rapid-Eye Mount
REMIR	REM IR camera
ROSS	REM Optical Slitless Spectrograph
RUCA	Rueda Cachanilla
SPM	San Pedro Mártir Observatory
SPSS	Spectro-Photometric Standard Star
TNG	Telescopio Nazionale Galileo
UT	Universal Time
VLT	Very Large Telescope (ESO)
VST	VLT Survey Telecope

Contents

1 Introduction

The Absolute calibration of the Gaia spectro-photometric data is based on a set of spectro-photometric standard stars (SPSS, see GA-001; GA-003) as described in the calibration model by PMN-003. A variety of instruments/telescopes, listed in Table 2, is used for the ground based observations of the SPSS (see LF-001, GA-002 for more details).

TABLE 2: Telescopes/Instruments used in the absolute calibration programme of the Gaia spectro-photometric data

Telescope	Instrument	Location	Ref.
Cassini 1.5m	BFOSC	Loiano, Italy	Sec. 4
ESO NTT 3.58m	EFOSC2	La Silla, Chile	Sec. 5
TNG 3.58m	DOLoRes	Roque de los Muchachos, Canary Islands, Spain	Sec. 6
CAHA 2.2m	CAFOS	Calar Alto, Spain	Sec. 7
REM 0.6m	ROSS(REMIR)	La Silla, Chile	Sec. 8
SPM 1.5m	LaRuca	Sierra San Pedro Mártir, Mexico	Sec. 9

Since we are interested in accurate and precise spectrophotometry, we investigated the instrumental effects that may affect the measurement, as the shutter effects and the CCD linearity, briefly described in Section 2, 3. The aim is to determine the observational requirements to get flux table with an error of a few per cent $(1 - 3\%)$. The analysis and the results obtained are reported in separate sections for each telescope/instrument, as shown in Table 2, fourth column. A synthetic summary of the results is shown in Table 12.

2 Shutter effects

Due to the finite opening and closing time of shutters, the effective exposure time of an astronomical frame might be slightly different from the settled value or may vary across the CCD. The offset between the requested exposure time and the effective value is known as the shutter delay time or shutter offset. It can be measured for example by taking a series of flat fields with increasing exposure time, starting from very short values for which the effect is more relevant. The frames must be trimmed and processed by subtracting overscan and/or bias, as described in SMR-001. In order to reduce the noise and to get rid of spurious effects, multiple images with the same exposure times are generally taken (usually triplets) and combined.
Of course the lamp must be stable or vary slowly enough so that the luminosity drift, monitored with flat fields sequences with constant exposure time, can be corrected as described in Section 2.1.
The frames of each triplet are used to build a single median frame for each exposure time and for each set of images with constant exposure time taken to check the lamp stability.
We used two different methods to estimate the shutter delay, as described in Section 2.2. Sec-

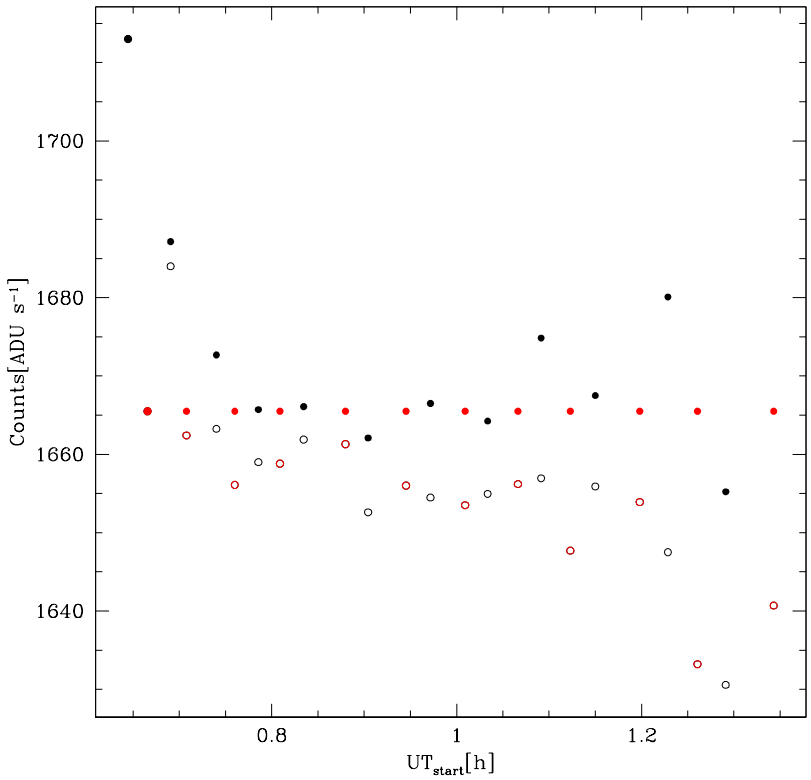

FIGURE 1: Example of real Counts/sec of flat fields obtained with different exposure times. The red empty dots represent the constant exposure time frames (10 sec) acquired to monitor the lamp stability (the fixed exposure time allow us to neglect possible shutter or linearity effects). In an ideal case the Counts/sec should not vary with time (in the x axis). The plot shows that the lamp is quite slow: this allows us to perform a good correction of the other frames, using the monitoring frames to scale properly the images. The black empty dots are the Counts/sec of the frames with varying exposure time. The filled dots are the Counts/sec corrected for the lamp variability. As expected the red dots are aligned, in an ideal case the black dots should be on the same line, in a real case there is some scatter. It is interesting to note, however, that this lamp is quite stable (the variation are of the order of ± 20 counts, i.e. $\sim 1.2\%$, excluding bigger variations corresponding to exposure times shorter than 4 sec, for which shutter effects become dominant. Data from LaRuca@1.5m, San Pedro Mártir Observatory (run V-006, 23 August 2008).

tion 2.3 describes a method to check exposure time variations across the CCD and to the estimate the minimum acceptable exposure time to get homogeneously illuminated images.

2.1 Lamp stability

The intensity and/or colour of the lamps used to acquire dome flat fields may vary with time for several reason. The most common reason is a thermal drift, which may produce an increase or decrease of the intensity with time. Frames with constant exposure times taken between images with varying exposure time, can be used to check the lamp stability and correct the images taken soon after (or soon before). All monitoring frames should be divided by a frame assumed as reference (for example the first one). In the ideal case (stable lamp) the result will be constant and equal to 1, in a real case their ratio will vary around 1. If the variations are slow and regular enough, the frames with varying exposure time can be corrected for the drift by dividing them by the ratio mentioned above (see Fig. 1).

2.2 Shutter delay

We used two different methods to estimate the shutter delay, as described in Sections 2.2.1 and 2.2.2.

2.2.1 Shutter delay - method #1

The mechanical shutter delay is determined by linear extrapolation at zero ADU (Analog-to-Digital Unit[1]) of the *linearity curve* (observed counts versus exposure time), thus assuming the response of the CCD is linear over the counts range used for the linear fit (see Fig. 2, upper panel). In the ideal case the linear extrapolation of the data should pass through the origin of the axis $(0, 0)$, but the fit of real data crosses the exposure time axis at a value $t \neq 0$ which represents the delay to be subtracted to correct all the exposure times.

2.2.2 Shutter delay - method #2

In theory the counts/sec should be constant for all exposure times over the linear range of the CCD, but real data might show deviations at short exposure times. We assume that the apparent deviation from linearity at low intensity is due to shutter effects, while the deviation from linearity at high intensity is intrinsic. The mechanical shutter delay is determined by adjusting the exposure times computing $t + \delta t$ by varying δt in a suitable range (from negative to positive values). The correct shutter delay δt to be applied is the one that produce a constant count rate for all the exposure times or, in other words, that minimize the residual from a horizontal line fitting all the points (see Fig. 2, lower panel).

Once known, the shutter delay can be used to correct the exposure times but is is usually negligible for long exposure times. A 10 ms shutter offset corresponds to a 1% error in a one sec. exposure, but the relative effect decreases with longer exposure times. We stress the fact that

[1] ADU can be converted to photoelectrons through the gain $[e^-/ADU]$.

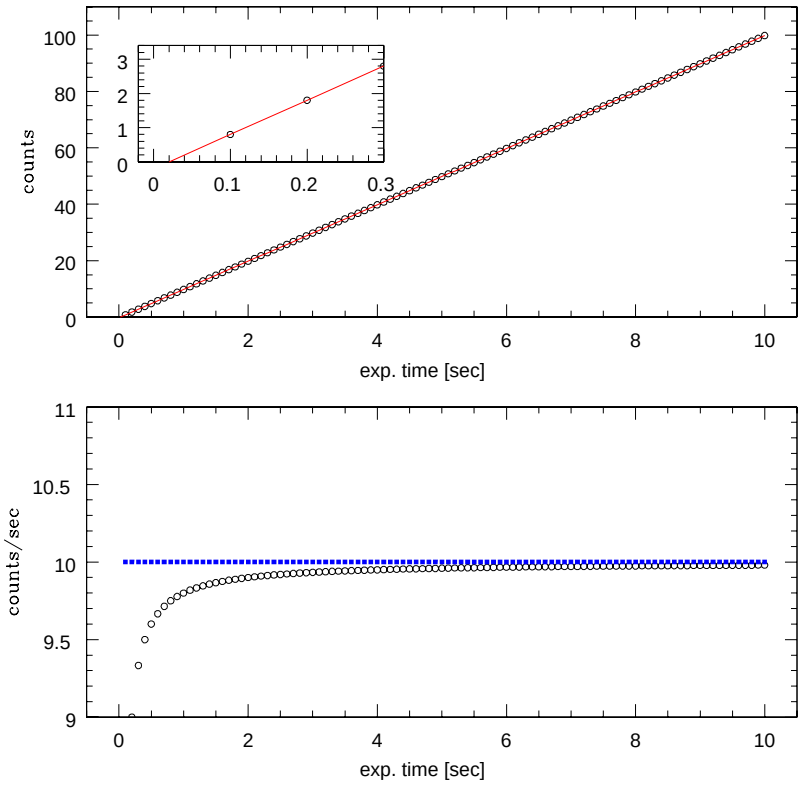

FIGURE 2: In this example, based on fictitious data, the nominal exposure times have been reduced by 0.02 sec. The upper panel shows how the linear extrapolation (red line) of the counts at zero ADU crosses the exposure time axis at $t = 0.02$ sec, as highlighted in the box, corresponding to $\delta t = -0.02$ sec, where the correct exposure time is $t = t_{exp} + \delta t$. The lower panel shows the counts/sec (black circles) computed with the same fictitious data as before. The most constant distribution as possible (blue squares) is obtained applying $\delta t = -0.02$ sec. In this case the error can be estimated from the residual scatter of the corrected points (zero in this ideal case) by dividing the points rms by their average counts rate.

flat fields acquired with too short exposure times and used to correct all frames of one night, will affect also the scientific images taken with relatively long exposure times.
Because shutter delay effects are usually negligible for long exposure times and because long exposure times usually correspond to high count levels, linearity tests are not so affected by shutter delay, because deviations from linearity are usually prominent at high count levels. Vice versa, since deviations from linearity are more evident at high counts, shutter delay test based on relatively short or very short exposure times, usually corresponding to low counts, are not so affected by deviations from linearity. This allows us to perform the test independently. However when deviations from linearity are particularly evident, we also applied a linearity correction to the shutter delay tests and vice versa.

2.3 2-D exposure time variations

A mechanical shutter can also produce exposure time variations across the CCD. This effect depends on the shutter type and on its quickness: the shutter takes a finite time to travel from fully closed to fully open and vice versa. In short exposures this can produce a significantly non uniform exposure of the CCD. To avoid this problem a moving slit type shutter can be used[2].
The shutters which are commonly used in many astronomical instruments are iris type shutters As an example, an iris type shutter can affect short exposure images as shown in Fig. 3, where it is clearly visible that the central part of the frames is exposed for a time longer than at the edges and the iris structure becomes evident. This image is obtained by dividing a flat field acquired

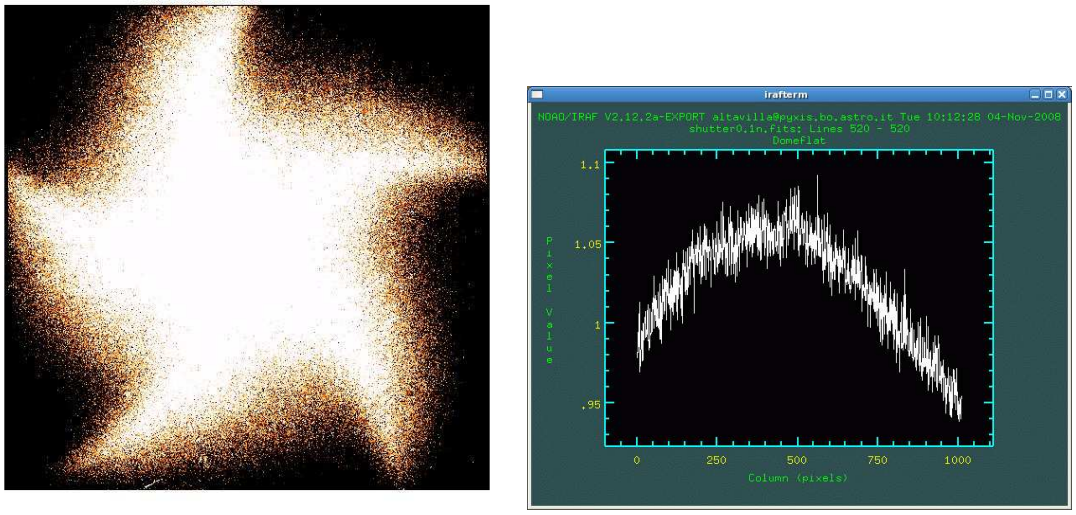

FIGURE 3: Left image: normalized ratio between a 0.1 sec and a 20 sec unfiltered dome flats taken on August 20, 2008 with LaRuca@1.5m. Right image: counts along a central line of the same frame, ADU variations of $\pm 10\%$ are visible.

with a very short exposure time by a reference one taken with a relatively long exposure time. The ratio is eventually normalized to the mean. In this case we do not care about the lamp stability, since we are interested only in the two-dimensional structure of the ratio and not in the absolute level of the counts. The structure of the ratio of flat fields with increasing exposure times (starting from very short times) with respect to a flat with a long exposure time (long enough to be reasonable safe from shutter effects) can give an estimate of the minimum exposure time for which the CCD illumination is flat enough for our purposes. In our case we look for 2-D variations $\leq 1\%$.
It is interesting to note that this effect can be interpreted as a shutter delay varying over the

[2] A moving slit type shutter, such as the *Bonn Shutter*, consists of two blades which move over the shutter aperture. The slit width and the blades speed are set to ensure a homogeneous illumination of the detector for each exposure time. Limitations are mainly due to the stepper motor resolution and the tolerances of the mechanics. A *Bonn Shutter* is used with BUSCA (the Bonn University Simultaneous CAmera) at the 2.2m telescope at CAHA and with OmegaCam at the VLT Survey Telecope (VST). More information can be found in `http://www.astro.uni-bonn.de/~ccd/shutters/shutter_general_info.php`.

frame. The effect is similar to the pure shutter delay (i.e. the average counts level of a flat field is smaller/larger than expected) but since there is a 2-D variation, it can not be corrected by simply adding a constant to the exposure time[3] but it can be removed by evaluating the $\delta_t(x, y)$ map from ratio images like the one in Fig. 3 and normalizing all frames to the nominal exposure time. We prefer the first approach, that is to set a minimum exposure time to neglect shutter effects, since it seems a more straightforward and safe approach to perform our observations and reduce our data.
While the shutter delay is usually very small, if any ($\delta t \ll 1$ sec), the minimum exposure time given by this test can be much larger, also of the order of a few seconds, so it must be considered more stringent than the shutter delay test results.

2.4 Shutter effects - Conclusions

The tests described in Sections 2.2.1, 2.2.2 allowed us to compute the value to be used to obtain the effective exposure time for a given instrument, or to define a minimum exposure time for which the shutter delay represents a negligible correction ($\leq 1\%$).

The test described in Section 2.3 is important to define the minimum exposure time that can be used observing with a given instrument/CCD in order to get homogeneously illuminated images. We define a *minimum acceptable exposure time* the value that produce a frame homogeneously illuminated (within 1%).
A summary of the results can be found in Section 10.

3 CCD linearity

Linearity is a measure of how consistently the CCD responds to different light intensity over its dynamic range. For example, if a 1 sec exposure to a stable light source produces 100 ADU, 10 sec should produce 1000 ADU[4], thus increasing linearly with exposure time. CCDs can exhibit non-linearities, typically at either or both low and high signal levels. High quality CCDs show significant deviations ($\geq 1\%$) from linearity only close to saturation, i.e. at high signal levels when the potential well depth is almost full. Of course CCDs strongly deviate at saturation, when the well depth is full and additional incoming photons do not increase the photoelectrons in a given pixel. Saturation is usually accompanied by blooming, i.e. the additional charge spreads into neighbouring pixels, usually along lines or columns depending on the CCDs structure (Fig. 4). A linear response of the CCD however is given not only by the photoelectron collection process but also by the transfer, amplification and readout processes. With high-

[3] The same plot and the same result shown in Fig. 2 can be obtained if we assume a frame to be illuminated one half for a time $t + \delta t_1$ and one half for a time $t + \delta t_2$ where $\delta t_1 = 0$ sec and $\delta t_2 = -0.04$ sec. Even applying the effective (average) exposure time delay correction $\delta t = -0.02$ sec, the image gradient will not be removed. In this example the gradient will be negligible ($\leq 1\%$) for exposure times $t \geq 4$ sec.

[4] Of course the intensity level must be measured on bias/overscan/dark corrected images.

performance sensors intended for scientific applications, considerable effort is made to ensure a linear relationship between incident photon level and output signal from the CCD. When observations are restricted to the linear portion of the full well capacity[5], the CCD performs as a detector suitable for accurate spectrophotometric measurements. The better is the linearity, the better is the calibration that can be achieved.
Two methods, based on photometric flat fields or spectroscopic flat fields, can be used to investigate the CCD linearity, as described in Section 3.1 and 3.2[6]. In both cases flat fields must be trimmed and processed by subtracting overscan and/or bias (and dark if necessary) as described in SMR-001. In order to reduce the noise and to get rid of spurious effects, multiple images with the same exposure time are taken (usually triplets) and combined. For our purposes we look for the intensity range corresponding to a negligible deviation from linearity ($\leq 1\%$).

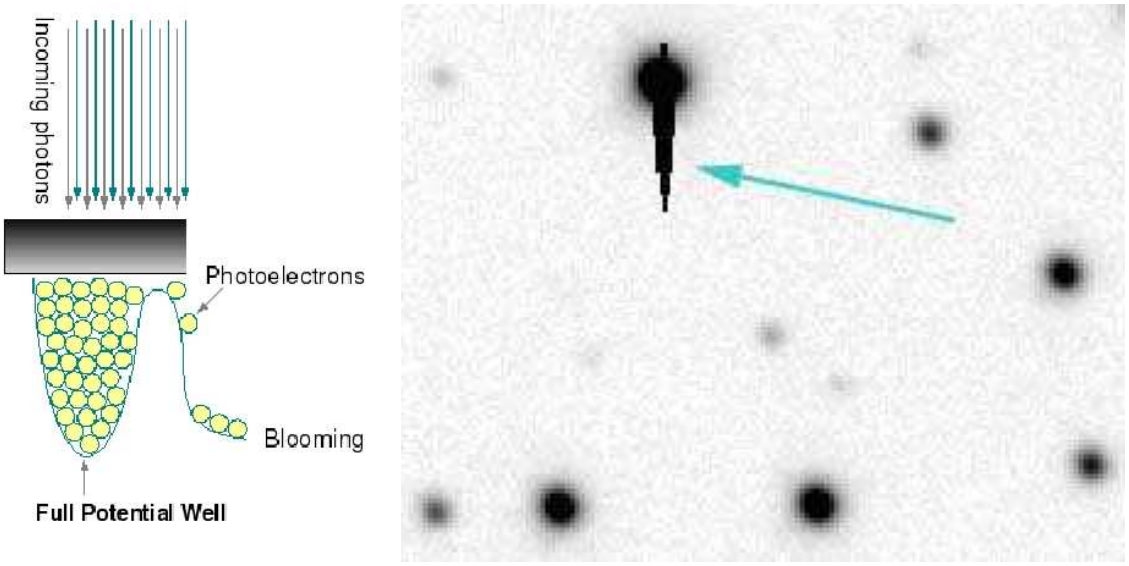

FIGURE 4: Left panel: cartoon of the vertical structure of a pixel full well capacity describing the saturation/blooming effect. Right panel: a real example of blooming.

3.1 Classical method

The "classical" method for measuring the CCD linearity consists in building a plot with ADU versus exposure time (corrected for shutter delay, if necessary, see Section 2). This test requires photometric flat field images with increasing signal (from faint to saturation). This can be simply achieved by taking a sequence of flat fields with increasing exposure time. Because the light source stability is crucial, the sequence must include reference images taken with fixed exposure time, to monitor the lamp stability and to correct for small and slow flux variations

[5]The amount of charge that can be accumulated in an individual pixel before saturation.
[6]Other methods can be devised or found in literature, as the *ratio method*, Baldry (1999) or the method described by Leach et al. (1980) but the two explored here are sufficient for our purpose.

as described in Section 2.1 (for this reason this method is also known as the *bracketed repeat-exposure method*). In the ideal case, CCDs will produce a plot where the ADUs increase linearly with exposure time. In general the high signal counts close to saturation will deviate from the linear fit of the points in the linear regime (i.e., points related to frames far from saturation and with long enough exposure times to avoid significant shutter effects). The deviation, better visible in a plot showing the residuals of the data from the linear fit, will provide a measurement of the non linearity. In particular, we are interested in determining the full well capacity range (in ADU) characterized by deviations from linearity $\leq 1\%$, (see Fig. 5).

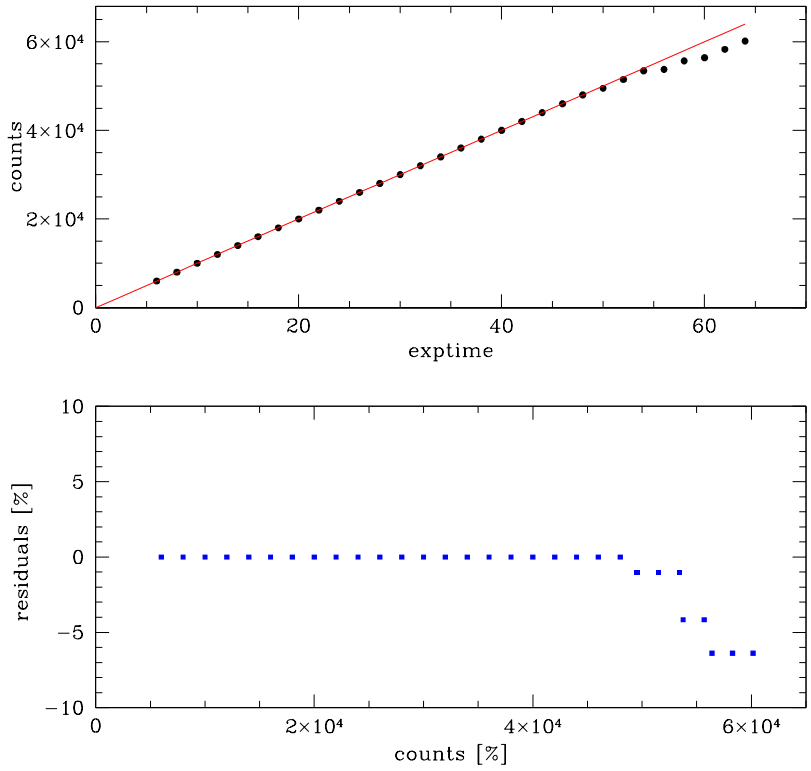

FIGURE 5: In this example, based on fictitious data, the expected counts at high signal have been arbitrarily reduced to simulate a non linearity response. The upper panel shows how the linear fit of the points in the linear regime (red line) does not match the simulated points at high signal. The lower panel shows the residuals [%] of the points from the expected values. The deviation from linearity becomes larger than 1% above 55000 ADU.

3.2 Stello's method

A second method for obtaining the linearity profile of the CCD response is described by Stello et al. (2006)[7]. In this case the required frames are at least two spectroscopic flats, one reaching

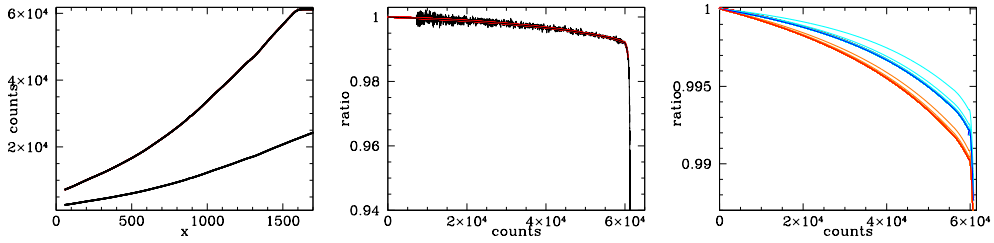

FIGURE 6: Left panel: combined spectroscopic flat field (collapsed to one-dimensional). The saturation limit is reached in the longest exposure time image. Middle panel: gain-ratio curve (see text). A red line show the result after replacing the noisy curve with a polynomial fit. The curve has also been extrapolated to intensity zero. Before starting the iterative procedure the resulting curve was multiplied by a suitable factor in order to be 1 at 0 ADU. Right: R_i iteration (cyan line) converges (blue line) on R_1 (in black but hardly seen because matched by the final iterated line) while G_i (orange line) converges on the actual gain curve (in red). The examined CCD is linear within 1% up to 60000 ADU,i.e. almost up to saturation, when the linearity shows a steep drop.

the saturation level and the other covering a fainter intensity range. The slit and grism used for the test are not crucial, the important thing is to get spectroscopic flat fields with a wide intensity range along one direction (column or line). A smooth monotonic variation from the minimum level to the peak is preferred but not crucial.

All frames must be collapsed to one-dimensional images by averaging them across dispersion[8] (see Fig. 6, left plot). As in the "classical" method, lamp luminosity (thermal) drifts must be corrected by scaling the one-dimensional collapsed frames by the ratio between the control images taken before or after each spectral flat. In this case the ratio of the collapsed control sequence frames may show not only flux variations but colour variations too.
The one-dimensional images, once corrected for lamp drifts if necessary, are used to compute the ratio corresponding to pairs with different exposure times, normalized by their exposure time:

$$R_1 = \frac{I_{t1}/t1}{I_{t2}/t2} \tag{1}$$

In an ideal case this ratio should be equal to one, the real case is shown in Fig. 6, middle panel. R_1 was fitted by a polynomial in order to get rid of the noise, extrapolated to zero ADU and forced to be 1 at 0 ADU by multiplying it by a suitable factor, as required by this method.
The so called *gain-ratio curve* R_1 is used as a first estimate of the actual underlying gain curve

[7] We thank D. Stello for clarifications about his method.
[8] This operation can be done with the IRAF task `blkavg`.

$G(I)$ to start the following iterative process:

$$G_1 = R_1 \tag{2}$$

$$R_2 = \frac{G_1(I)}{G_1(I \cdot t_2/t_1)} \tag{3}$$

where in this example $t_1 = 55$ sec, $t_2 = 20$ sec and $I = I_{55}$,

$$G_2 = \frac{R_1}{R_2} G_1 \tag{4}$$

and continuing the iterative process:

$$R_i = \frac{G_{i-1}(I)}{G_{i-1}(I \cdot t_2/t_1)} \tag{5}$$

$$G_i = R_1/R_i \cdot G_{i-1}. \tag{6}$$

until R_i matches R_1, as shown in Fig. 6, right panel. The corresponding G_i represents the linearity curve of the CCD.

3.3 CCD linearity - Conclusions

The test described in Section 3.1 and 3.2 allow us to define the maximum level (ADU) for which a given CCD produce a linear response. In particular, we look for the intensity range corresponding to a negligible deviation from linearity ($\leq 1\%$ for our purposes).
The *classic method* (Section 3.1) maps the CCD dynamic range with a number of points proportional to the number of photometric flat fields acquired, hence a large number of frames is desirable to get a good coverage of the CCD linearity.
The *Stello's method* (Stello et al. 2006 and Section 3.2) can be performed in principle with two spectroscopic flat fields only and it maps the whole CCD dynamic range with a continuous sampling. On the other hand this method seems very sensitive to the input data and to their treatment.
We use the first or the second method, or both, according to the available data. A summary of the results can be found in Section 10.

4 BFOSC@Cassini 1.5m

4.1 BFOSC Shutter effects

We tested the CCD EEV 1300×1340B (new[9]) mounted at BFOSC for shutter effects. We used 86 dome-flats (B band) acquired to this aim on May. 27, 2009 (run V-011). The statistics of the frames are given in Table 2. We used the method described in Section 2.1 to check the stability of the lamp used for the dome flats. As shown in Fig. 7, left panel, the lamp flux is quite unstable with time. We used the methods described in Section 2.2.1 and 2.2.2 to compute the shutter delay.

[9]This is the new CCD mounted in July 2008 to replace the old EEV 1300 × 1340B. No data are available for the characterization of the previous CCD.

TABLE 3: Statistics of the B flat field used for the shutter delay test at Loiano

IMAGE	MEAN [ADU]	MODE [ADU]	STDDEV [ADU]	EXPT [sec]
r.may27_007.fits	4511.	4507.	157.2	5.0
r.may27_008.fits	4479.	4494.	156.1	5.0
r.may27_009.fits	4494.	4504.	156.6	5.0
r.may27_010.fits	3352.	3370.	119.	4.0
r.may27_012.fits	3318.	3322.	117.7	4.0
r.may27_013.fits	4216.	4221.	147.2	5.0
r.may27_014.fits	4210.	4203.	147.1	5.0
r.may27_015.fits	4491.	4497.	156.5	5.0
r.may27_016.fits	8245.	8233.	281.	10.0
r.may27_017.fits	8298.	8293.	282.8	10.0
r.may27_018.fits	8186.	8163.	278.9	10.0
r.may27_019.fits	4003.	4003.	140.4	5.0
r.may27_020.fits	4474.	4486.	155.9	5.0
r.may27_021.fits	4438.	4436.	154.8	5.0
r.may27_022.fits	2586.	2588.	93.89	3.0
r.may27_023.fits	2599.	2593.	94.39	3.0
r.may27_024.fits	2368.	2370.	86.66	3.0
r.may27_025.fits	4062.	4069.	142.2	5.0
r.may27_026.fits	4044.	4054.	141.6	5.0
r.may27_028.fits	1534.	1540.	59.63	2.0
r.may27_029.fits	1440.	1455.	55.63	2.0
r.may27_030.fits	1519.	1528.	59.03	2.0

TABLE 2: Statistics of the B flat field used for the shutter delay test at Loiano - continued

IMAGE	MEAN [ADU]	MODE [ADU]	STDDEV [ADU]	EXPT [sec]
r.may27_031.fits	4050.	4042.	141.9	5.0
r.may27_032.fits	4093.	4095.	143.3	5.0
r.may27_033.fits	4035.	4046.	141.3	5.0
r.may27_034.fits	649.1	655.9	33.18	1.0
r.may27_035.fits	618.8	626.3	32.36	1.0
r.may27_036.fits	600.7	611.6	31.74	1.0
r.may27_037.fits	3968.	3967.	139.1	5.0
r.may27_038.fits	4007.	4008.	140.4	5.0
r.may27_039.fits	4377.	4374.	152.8	5.0
r.may27_040.fits	208.3	222.4	23.46	0.5
r.may27_041.fits	151.9	162.8	21.79	0.5
r.may27_042.fits	163.6	174.	21.81	0.5
r.may27_043.fits	4191.	4180.	146.5	5.0
r.may27_044.fits	4237.	4249.	147.9	5.0
r.may27_045.fits	4177.	4187.	146.2	5.0
r.may27_046.fits	10280.	5447.	4795.	0.2
r.may27_047.fits	10598.	17419.	4858.	0.2
r.may27_049.fits	3947.	3940.	138.5	5.0
r.may27_051.fits	4364.	4368.	152.4	5.0
r.may27_052.fits	6320.	6313.	217.2	7.0
r.may27_053.fits	6234.	6242.	214.3	7.0
r.may27_054.fits	6275.	6282.	215.6	7.0
r.may27_055.fits	4325.	4317.	151.	5.0
r.may27_056.fits	4306.	4301.	150.4	5.0
r.may27_057.fits	4310.	4317.	150.4	5.0
r.may27_058.fits	18734.	18656.	630.2	20.0
r.may27_059.fits	18567.	18558.	624.6	20.0
r.may27_060.fits	18456.	18416.	620.9	20.0
r.may27_061.fits	4275.	4279.	149.3	5.0
r.may27_063.fits	4213.	4209.	147.3	5.0
r.may27_064.fits	27646.	27618.	926.6	30.0
r.may27_065.fits	28266.	28267.	947.3	30.0
r.may27_066.fits	28110.	28016.	942.1	30.0
r.may27_067.fits	4701.	4692.	163.4	5.0
r.may27_068.fits	4791.	4791.	166.5	5.0
r.may27_069.fits	4766.	4768.	165.6	5.0
r.may27_070.fits	38249.	38071.	1279.	40.0
r.may27_071.fits	38328.	38233.	1281.	40.0

TABLE 2: Statistics of the B flat field used for the shutter delay test at Loiano - continued

IMAGE	MEAN [ADU]	MODE [ADU]	STDDEV [ADU]	EXPT [sec]
r.may27_072.fits	38832.	38822.	1298.	40.0
r.may27_073.fits	4795.	4778.	166.6	5.0
r.may27_074.fits	4669.	4672.	162.4	5.0
r.may27_075.fits	4632.	4633.	161.2	5.0
r.may27_076.fits	56417.	56283.	1875.	60.0
r.may27_077.fits	54971.	54720.	1829.	60.0
r.may27_078.fits	56678.	56414.	1883.	60.0
r.may27_079.fits	4677.	4676.	162.6	5.0
r.may27_080.fits	4666.	4668.	162.3	5.0
r.may27_081.fits	4646.	4657.	161.6	5.0
r.may27_082.fits	47232.	46991.	1576.	50.0
r.may27_083.fits	47383.	47098.	1581.	50.0
r.may27_084.fits	46902.	46767.	1565.	50.0
r.may27_085.fits	4850.	4862.	168.4	5.0
r.may27_086.fits	4848.	4847.	168.4	5.0
r.may27_088.fits	54452.	54157.	1812.	55.0
r.may27_089.fits	54336.	54206.	1809.	55.0
r.may27_090.fits	54133.	54092.	1802.	55.0
r.may27_091.fits	4768.	4756.	165.8	5.0
r.may27_092.fits	4578.	4587.	159.5	5.0
r.may27_093.fits	4571.	4576.	159.2	5.0
r.may27_094.fits	4726.	4716.	164.3	5.0
r.may27_095.fits	61402.	61127.	2024.	65.0
r.may27_096.fits	61325.	61046.	2022.	65.0
r.may27_097.fits	61278.	61167.	2021.	65.0
r.may27_098.fits	61520.	61276.	2028.	65.0

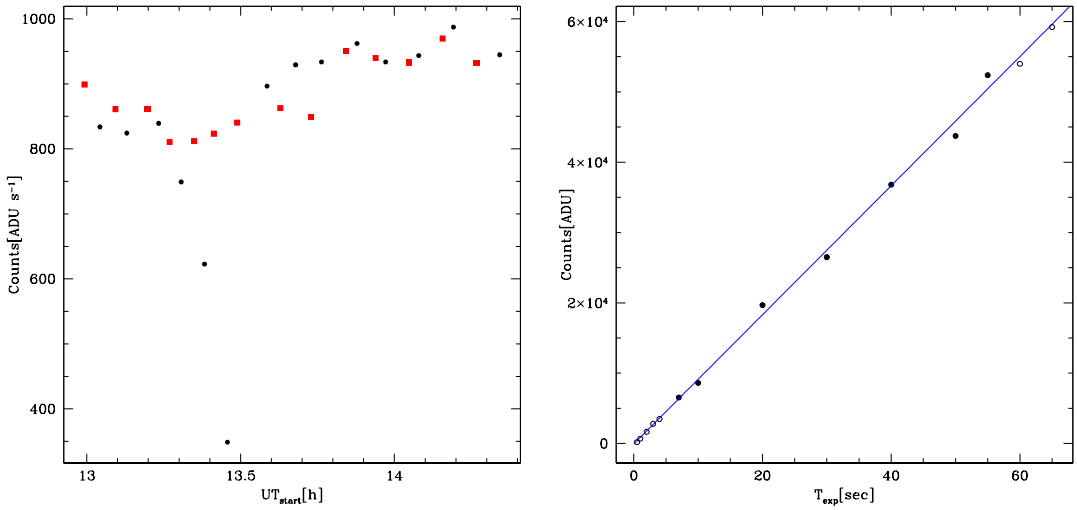

FIGURE 7: Left Panel: Counts/sec of the median flats per given exposure time obtained from the frames listed in Table 2. Flat fields triplets with the same exposure time have been combined into single median images. The red filled squares represent the 5 sec flats acquired to monitor the lamp (the fixed exposure time allows us to neglect possible shutter or linearity effects). It is evident that the lamp is quite variable. This fact does not allow us to perform a good correction of the other frames, even using the monitoring frames to scale the images. Right panel: shutter delay obtained from the data in Table 2, selecting the points with $5 < t \leq 55$ sec (filled dots, counts lower than 55000 ADU). The linear extrapolation to zero ADU of the observed counts (corrected for the lamp drift) vs. exposure time, crosses the time axis at $t = +0.06$ sec. The corresponding shutter delay to be summed to the exposure times is $\delta_t = -0.06 \pm 1.29$ sec.

The analysis of the data with the first method (Section 2.2.1) gives a shutter delay of $\delta_t = -0.06 \pm 1.29$ sec (Fig. 7, right panel). The results is quite uncertain, probably because of the lamp instability.
We tried to compute the shutter delay also with the second method (Section 2.2.1), as shown in Fig. 8. In this case $\delta_t \simeq -0.3$ sec. In both methods, data have been limited to exposure times shorter than 55 sec, i.e. intensity lower than $\simeq 55000$ ADU, to avoid possible strong deviation from linearity effects.

We also looked at the 2-D images, trying to determine the minimum exposure time needed to avoid possible illumination inhomogeneities as described in Section 2.3. Fig. 9 shows the ratio between B dome flats taken on May 27, 2009 with BFOSC (run V-011). We computed the ratio with respect to the 50 sec master flat. We assumed that 50 sec are enough to avoid shutter effect an that the corresponding average counts, 47000 ADU, are safe from significant deviations from linearity, as also visible in Fig. 7. Exposure times shorter than 4 sec produce significant illumination inhomogeneities, that decrease from $\sim 30\%$ (in the 0.5 sec frames) to less than 2% in the 4 sec frames and $\leq 1\%$ in the 5 sec frames. The 65 sec frames (61000 ADU) show a very slight depression in the centre of the frame, probably due to linearity deviations,

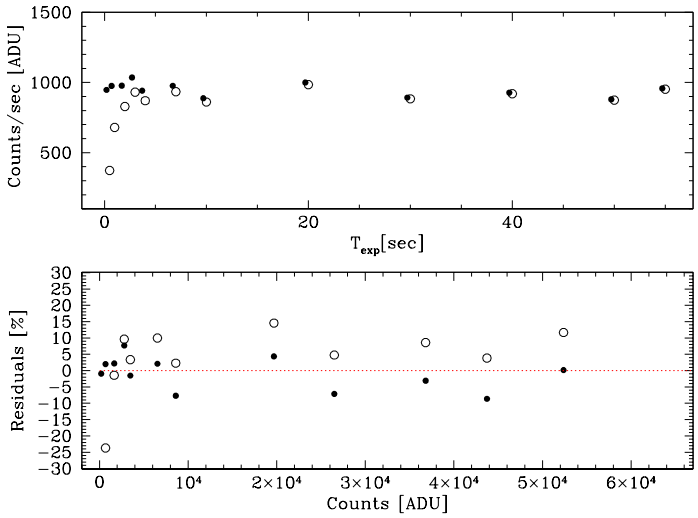

FIGURE 8: Shutter delay obtained from the data in Table 2, neglecting the points with $t > 55$ sec. Flat fields with the same exposure time have been combined into a single median image. Upper panel: count rates vs. exposure time. Lower panel: residuals of the count rates from their average value. Empty dot are the uncorrected values; filled dots are the data corrected for shutter delay. The scatter from the horizontal line is minimized with $\delta_t = -0.30 \pm 0.05$ sec (to be summed to the exposure times).

although barely visible and well within 1%.

Our results suggest not to use exposure times shorter than $\simeq 5$ sec if a homogeneous illumination of the frame is needed. The same data show that the effective exposure times are 0.3 sec shorter than the requested values, but this value is probably an effect of the 2-D exposure time variation rather than a simple shutter delay. The 2-D gradient visible in Fig. 9 in fact cannot be corrected by computing an effective exposure time. No strong evidence of deviations from linearity is visible with the data shown in this section. The last two conclusions are weakened by the lamp instability that does not allow us to get firm results.

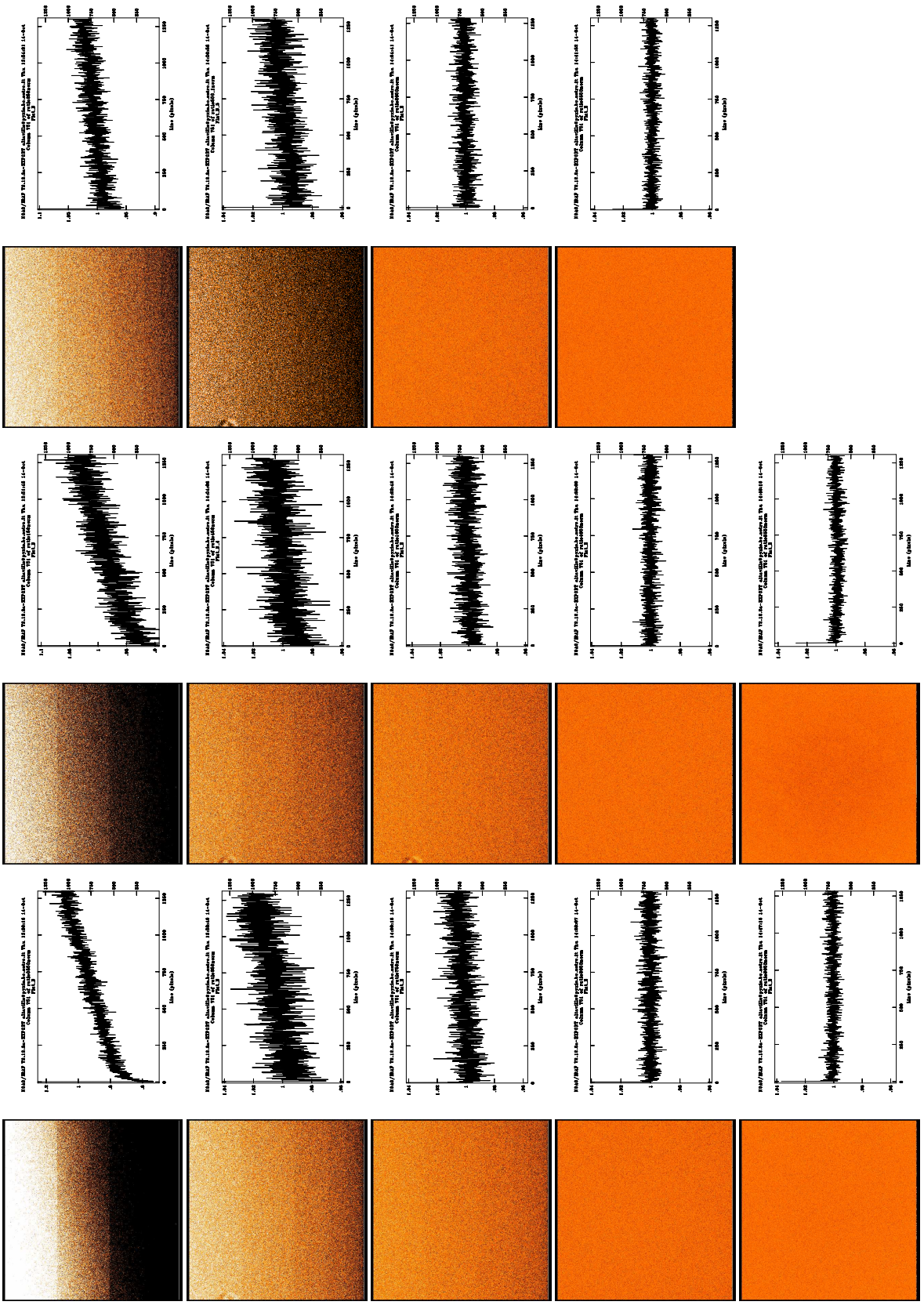

FIGURE 9: Normalized ratio between the V band masterflats with exp. time (from left to right, from the top to the bottom) equal to 0.5, 1, 2, 3, 4, 5, 7, 10, 20, 30, 40, 55, 60 and 65 sec with respect to the 50 sec exp. time masterflat. Colour cuts are the same for all images (z1=0.9 z2=1.1). The trace of the central column is shown on the right of each 2-D image. Data taken on May 27, 2010.

4.2 BFOSC CCD linearity

Our aim is to check the linearity of the response of the CCD EEV 1300×1340B (new) [10] mounted on BFOSC@Cassini 1.5m, We used the method for obtaining the linearity profile of the CCD response described in Section 3.2.
On Aug 30 2010 (run V-021) we obtained spectroscopic dome flats using the following instrumental setup: grism 7, slit 2.0 arcsec. Details of the combined images are shown in Table 3 Our instrumental setup allows us to obtain images with a wide intensity range, with a smooth variation from the minimum level to the peak, suitable for our purposes (see Fig. 10).

TABLE 3: Statistics of the spectroscopic flat field (gr. 7, slit 2 arcsec) used for the linearity test at Loiano

N images	Exp. time [sec]	Counts⋆ [ADU] min	max	UT start†
3	10	0.999	26432.	21:38:33
3	6	1.	15937.	21:41:29
3	10	0.	25904.	21:43:16
3	26	1.998	65433	21:46:09
3	10	1.006	25864.	21:49:27

⋆ values measured on the combined image (median) of each set.
† value measured on the first image of each set.

First we checked the lamp stability along time (we took our data in about 10 minutes, see Table 3). Fig. 10, right panel, shows the ratio between each combined collapsed image with constant exposure time and the last one. The first set of control images shows that the lamp flux becomes unstable soon after the lamp is switched on. The second set of control images, taken about 5 minutes from the first, is more similar in shape and intensity to the last set of images. The flux variation can be taken into account while processing the images for the linearity test but it seems quite fast for a reliable correction (the results change significantly if the control images taken before or after each spectroscopic flat field are used to correct for the lamp drift).

The corrected images are then used according to the recipe described in Section 3.2 (the *Stello's method*), and the results are shown in Fig. 11.
The results do not change significantly if we apply a time delay correction by subtracting 0.3 sec to the nominal exposure time (see Section 4.1) since the shape of the ratio does not change significantly, but it is strongly affected by the lamp luminosity correction (see Fig. 12). Nevertheless, if we apply the time delay correction$= -0.3$ the mean value of the ratio, expected to be $\simeq 1$, changes significantly, (see Fig. 12), supporting the idea that this is not a shutter offset but an effect due to the inhomogeneous illumination of the CCD.

[10] This is the new CCD mounted in July 2008.

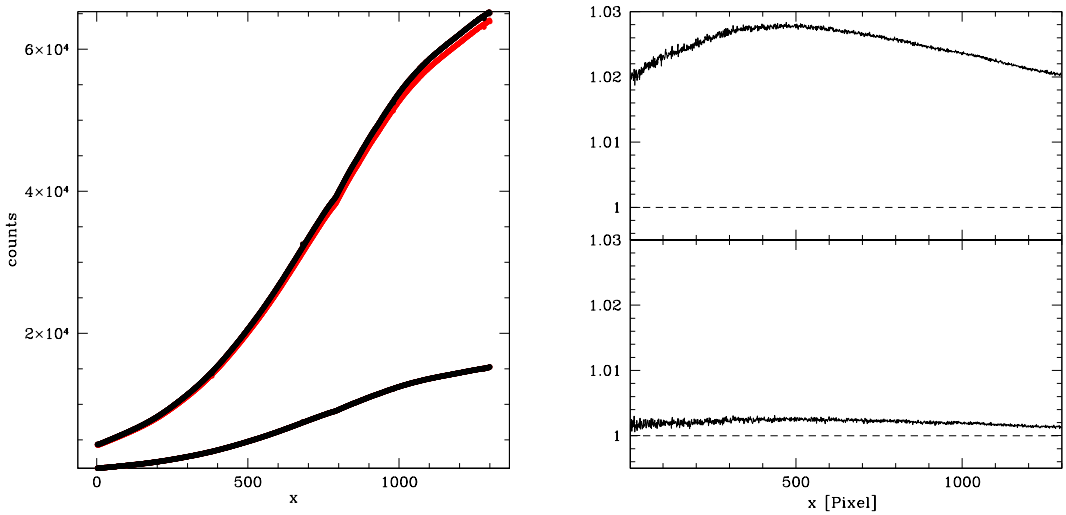

FIGURE 10: Left panel: Combined spectroscopic flat fields (collapsed to one-dimensional) obtained with BFOSC@Cassini 1.5m, grism 7, slit 2 arcsec. The two black curves correspond to flats acquired with exposure times of 26 and 6 sec (on 30 Aug 2010) corrected for the lamp luminosity drift. The red curves are not corrected for the lamp luminosity drift, (only the curve corresponding to the 26 sec exposure time is visible since the 6 sec corrected curve overlaps the uncorrected curve). Right panel: each panel shows the ratio between the first and the second control exposures (10 sec each) with respect to the third 10 sec image taken to monitor the lamp stability. A lamp dimming with time and a change in colour is evident (the x axis correspond to the wavelength range of the grism).

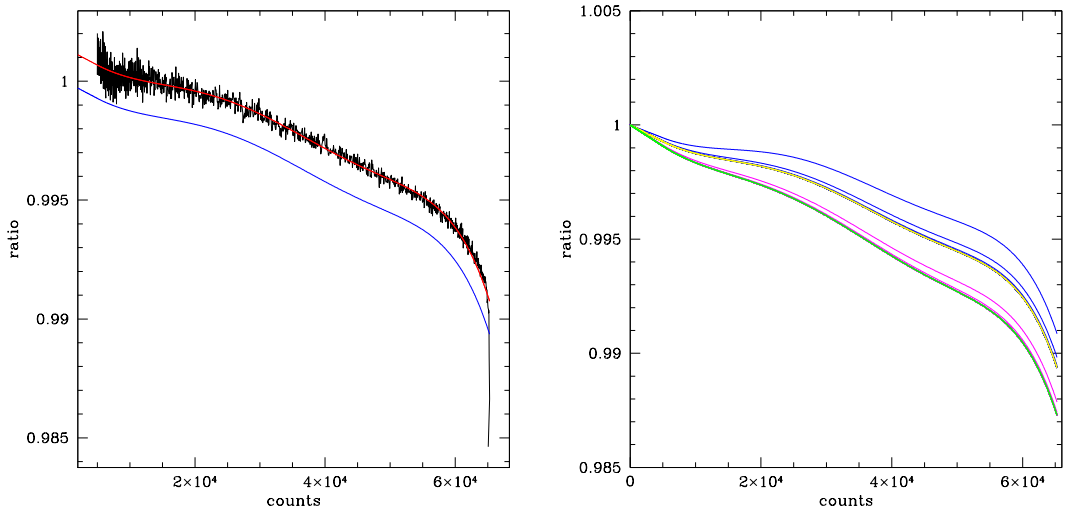

FIGURE 11: Left panel: ratio $R_1 = I_{26}/26/I_6/6$ vs. I_{26}; The 26 and 6 sec curves have been corrected for the lamp luminosity (thermal) drift (see Section 2.1). A red line shows the result after replacing the noisy curve with a polynomial fit (order 6). The curve has been extrapolated to intensity zero as well. Before starting the iterative procedure, the resulting curve has been multiplied by a suitable factor in order to be 1 at 0 ADU (blue curve). Right panel: R_i iteration (blue line) converges (yellow line) on R_1 (in black but hardly seen because matched by the final iterated line) while G_i (magenta line) converges on the actual gain curve (in green). The deviation from linearity is smaller than 1% up to $\simeq$ 60000 ADU.

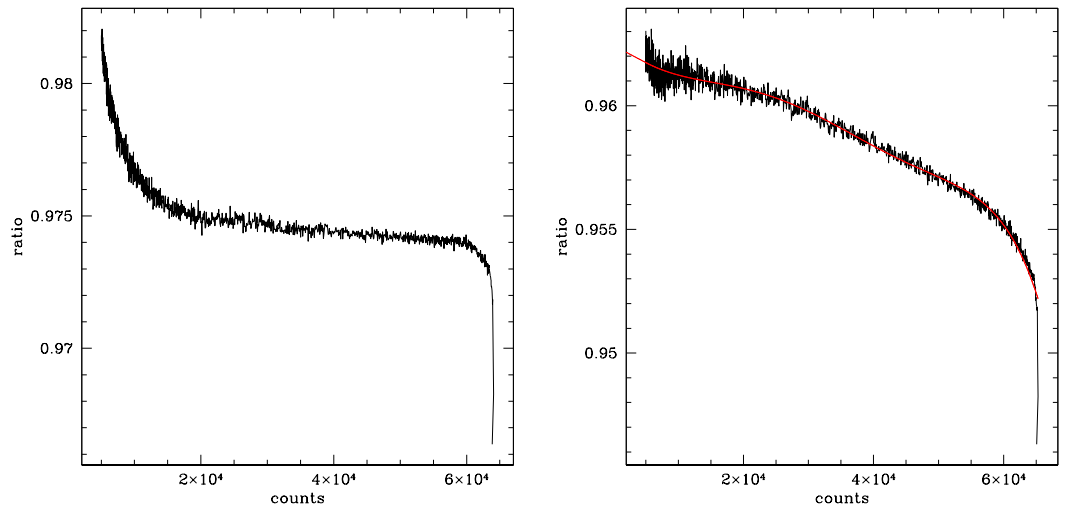

FIGURE 12: Left panel: like Fig. 11 (left panel), but without any lamp luminosity drift correction. Right panel: like Fig. 11 (left panel), with $\delta_t = -0.3$ sec time delay correction applied to the exposures times.

4.3 BFOSC Conclusions

A significant negative shutter delay $\delta_t \simeq -0.3$ sec has been measured with the test described in Section 4.1, based on data taken on May 27, 2009, but it seems not supported by the test in Section 4.2, based on data taken on Aug. 30, 2010.
Because of this discrepancy, we contacted the staff of the Astronomical Observatory of Loiano. R. Gualandi informed us that the shutter of BFOSC was changed in February 2010 and that the new one is *"much faster than the original shutter but affected by vignetting with exposure times faster than* $\simeq 4$ *sec"*, confirming our results and providing a reasonable explanation for the discordant results of our tests. Hence we assume $\delta_t \simeq -0.3$ sec for data taken before February 2010, and negligible (consistent with zero within the large uncertainty) afterwards.
2-D exposure time variations, i.e., non uniform CCD illumination, seem to be present for exposure times as large as $\simeq 5$ sec. Hence exposures times shorter than 5 sec should be avoided to get a homogeneous illumination of the CCD (within $\sim 1\%$).

The tests show that the new CCD EEV 1300×1340B deviation from linearity is smaller than 1% up to $\simeq 60000$ counts, afterwards the linearity deviation increases quickly. The results have been checked by correcting the spectroscopic flat fields for linearity and computing their ratio. Fig. 13 shows that, as expected from a correct linearity deviation correction, the ratio of the flat fields is flattened around 1.
No data are available for the linearity characterization of the old CCD EEV 1300×1340B but, because the old and the new CCDs are of the same model, we expect similar performances (for safety we can decrease the limit to 55000 ADU).

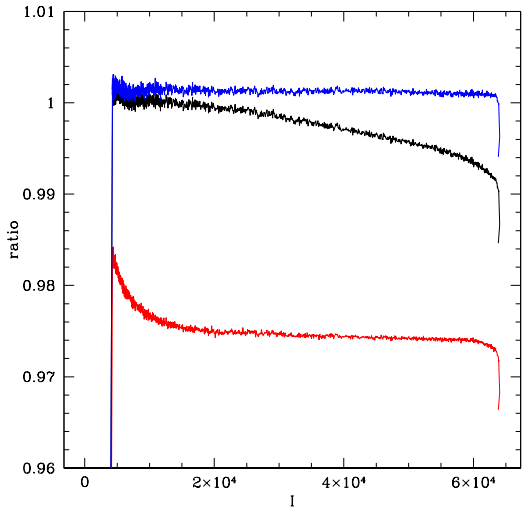

FIGURE 13: Ratio between the 26 sec and 6 sec spectroscopic flat fields without any correction (red line), after lamp drift correction (black line), after lamp drift and linearity correction (blue line). The steep increase of the ratio without any correction (red line) at low counts is due to the lamp drift.

5 EFOSC2@@NTT 3.58m

5.1 EFOSC2 Shutter effects

We tested the CCD#40 LORAL/LESSER detector mounted at EFOSC2 for shutter effects. We used the method described in Section 2 using data acquired to this aim on Nov. 28, 2008 (run M-007). The data consist of a series of 54 photometric dome flats (V band), with the statistics given in Table 4.

TABLE 4: Statistics of the B flat fields used for the shutter delay test at NTT

IMAGE	MEAN [ADU]	MODE [ADU]	STDDEV [ADU]	EXPT [sec]
EFOSC0349.fits	310.4	307.	21.98	0.1006
EFOSC0350.fits	305.7	306.9	22.62	0.1006
EFOSC0351.fits	301.6	304.9	21.45	0.1005
EFOSC0352.fits	28837.	29174.	1231.	10.0006
EFOSC0353.fits	28158.	28479.	1201.	10.0006
EFOSC0354.fits	28022.	28330.	1194.	10.0005
EFOSC0355.fits	592.7	592.4	126.3	0.2006
EFOSC0356.fits	581.2	580.5	33.4	0.2006
EFOSC0357.fits	580.3	581.2	33.4	0.2005
EFOSC0358.fits	28712.	29043.	1226.	10.0006
EFOSC0359.fits	28042.	28388.	1196.	10.0005
EFOSC0360.fits	27946.	28287.	1191.	10.0005
EFOSC0361.fits	1448.	1450.	128.	0.5006
EFOSC0362.fits	1415.	1428.	69.68	0.5005
EFOSC0363.fits	1408.	1425.	69.35	0.5006
EFOSC0364.fits	28664.	28998.	1224.	10.0006
EFOSC0365.fits	28032.	28389.	1196.	10.0005
EFOSC0366.fits	27937.	28282.	1191.	10.0005
EFOSC0367.fits	2871.	2892.	156.3	1.0006
EFOSC0368.fits	2805.	2825.	128.8	1.0005
EFOSC0369.fits	2787.	2809.	128.	1.0006
EFOSC0370.fits	28665.	29006.	1224.	10.0005
EFOSC0371.fits	28005.	28347.	1195.	10.0005
EFOSC0372.fits	27918.	28243.	1190.	10.0005
EFOSC0373.fits	5719.	5776.	253.6	2.0006
EFOSC0374.fits	5580.	5620.	247.3	2.0006

TABLE 4: Statistics of the B flat fields used for the shutter delay test at NTT - continued

IMAGE	MEAN [ADU]	MODE [ADU]	STDDEV [ADU]	EXPT [sec]
EFOSC0375.fits	5571.	5615.	241.8	2.0005
EFOSC0376.fits	28647.	28970.	1223.	10.0006
EFOSC0377.fits	27981.	28334.	1194.	10.0005
EFOSC0378.fits	27900.	28212.	1190.	10.0005
EFOSC0379.fits	8566.	8655.	370.1	3.0005
EFOSC0380.fits	8380.	8462.	363.	3.0005
EFOSC0381.fits	8331.	8413.	358.	3.0006
EFOSC0382.fits	28667.	29018.	1225.	10.0006
EFOSC0383.fits	28001.	28328.	1195.	10.0005
EFOSC0384.fits	27894.	28249.	1189.	10.0006
EFOSC0385.fits	17150.	17351.	733.9	6.0006
EFOSC0386.fits	16741.	16938.	717.6	6.0006
EFOSC0387.fits	16709.	16894.	717.	6.0006
EFOSC0388.fits	28664.	29023.	1225.	10.0006
EFOSC0389.fits	28031.	28387.	1196.	10.0006
EFOSC0390.fits	27943.	28297.	1191.	10.0006
EFOSC0391.fits	43140.	43627.	1875.	15.0006
EFOSC0392.fits	42153.	42688.	1835.	15.0006
EFOSC0393.fits	42078.	42539.	1832.	15.0006
EFOSC0394.fits	28656.	29014.	1220.	10.0005
EFOSC0395.fits	27993.	28325.	1191.	10.0006
EFOSC0396.fits	27917.	28228.	1188.	10.0006
EFOSC0397.fits	57637.	58225.	2422.	20.0006
EFOSC0398.fits	56423.	57092.	2373.	20.0006
EFOSC0399.fits	56265.	56976.	2366.	20.0006
EFOSC0400.fits	28662.	29002.	1220.	10.0006
EFOSC0401.fits	28022.	28330.	1192.	10.0006
EFOSC0402.fits	27931.	28250.	1188.	10.0005

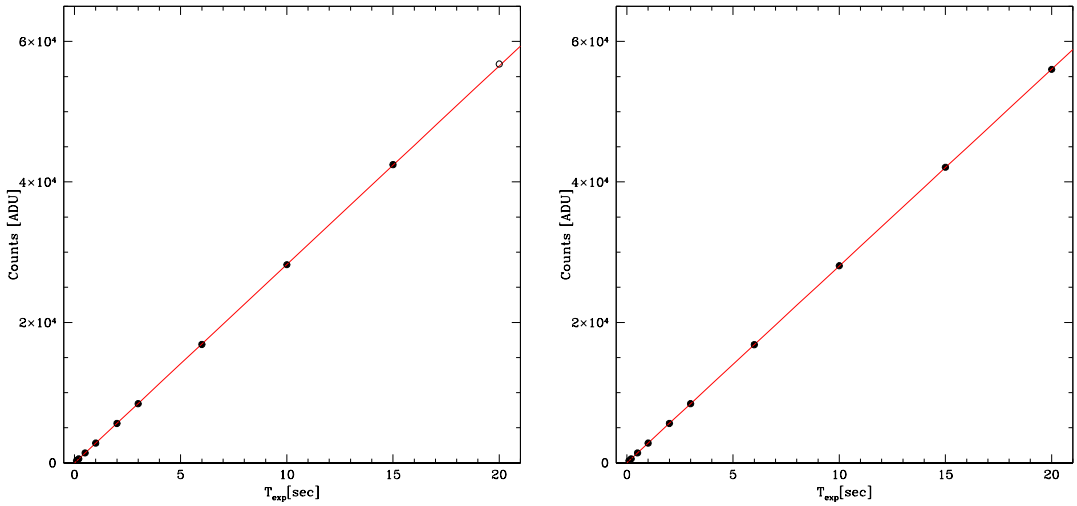

FIGURE 14: Left Panel: Shutter delay obtained from the data in Table 4, rejecting the points with $t \geq$ 20 sec (empty dot). Flat fields with the same exposure time have been median combined into single images. The linear extrapolation to zero of the observed counts vs. exposure time crosses the time axis at $t = 0.006$ sec. The corresponding shutter delay to be summed to the exposure times is $\delta_t = -0.006 \pm 0.008$ sec. Right panel: as before but with the linearity correction applied (see Section: 5.2), and without rejecting any point. In this case the linear extrapolation to zero ADU of the observed counts vs. exposure time crosses the time axis at $t = -0.009$ sec. The corresponding shutter delay to be summed to the exposure times is $\delta_t = 0.009 \pm 0.003$ sec.

The first method (Section 2.2.1) gives a shutter delay of $\delta_t = -0.006 \pm 0.008$ sec (Fig. 14). The results is opposite in sign with respect to the value $\delta_t = +0.008$ sec, obtained with the second method (Section 2.2.2, see Fig. 15) but consistent within 3σ. In both methods, data have been limited to exposure times shorter than 20 sec, i.e. counts lower than $\simeq 45000$ ADU.
If we apply the linearity correction (see Section: 5.2) and we make use of all data points, we obtain a shutter delay of $\delta_t = +0.009 \pm 0.003$ sec and $\delta_t = 0.008 \pm 0.001$ sec, respectively, from the two methods.

It is interesting to point out that Fig. 15 (left panels), shows an anomalous trend: the ADU rate increases with exposure time or, equivalently, with the intensity level. The first simple explanation, a lamp drift, was ruled out by the analysis of the frames taken to monitor the lamp stability during the shutter time test (Fig. 16, upper panel). The lamp stability test also shows that each triplet of frames has a decreasing ADU rate pattern: the first one being systematically brighter than the other two, but the pattern and the ADU rate do not change for each triplet. Nevertheless, the ADU rate of the frames acquired varying the exposure time does not show the expected constant trend (Fig. 16, lower panel[11]). While the increasing ADU rate toward short exposure times can be explained by the shutter delay (and it is effectively corrected assuming

[11] ADU levels in Fig. 16 are slightly higher than the values shown in Fig. 15 because the former plot is based on the frame mode value, the latter on their mean.

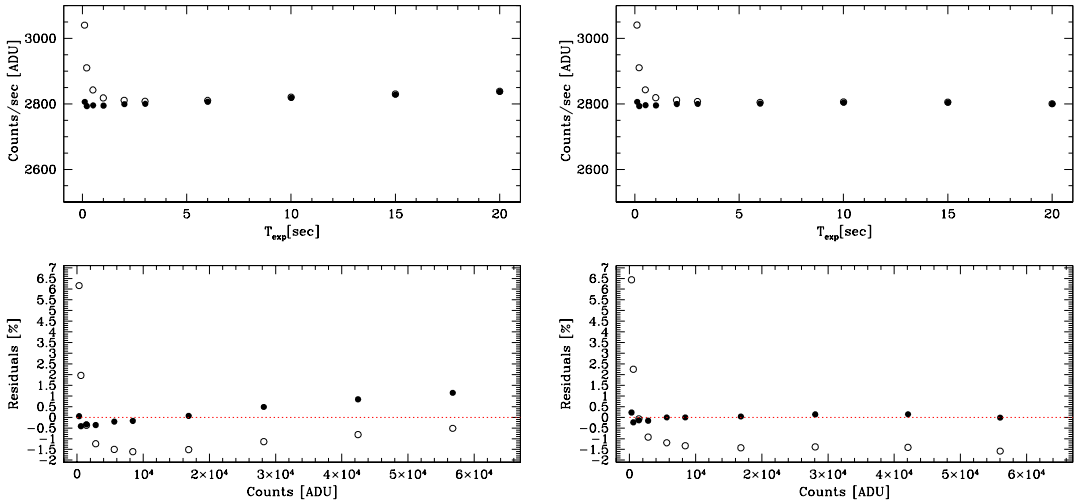

FIGURE 15: Left panel: shutter delay obtained from the data in Table 4, rejecting the points with $t \geq 20$ sec flat fields with the same exposure time have been median combined into a single image. Upper panel: count rates vs. exposure time. Lower panel: residual of the count rates from their average value. Empty dot are the uncorrected values; filled dots are the data corrected for shutter delay. The scatter from the horizontal line is minimized with $\delta_t = +0.008 \pm 0.005$ sec. Right panel: as before but with linearity correction applied and taking into account all data points (see Section: 5.2). The scatter from the horizontal line is minimized with $\delta_t = +0.008 \pm 0.001$ sec, as before.

$\delta_t = +0.008$ sec), the increasing trend towards large exposure times can not be easily explained without non linearity effects. The decreasing pattern of each triplet may be an effect of the observing modality: since the standard *Observing Blocks*[12] (OB) for acquiring photometric flats do not allow the user to set the exposure time (which is usually automatically computed according to the requested image intensity level), the shutter time test has been performed bypassing the system. Hence the lamp and its management can be different from the observing modality used acquiring photometric flats with the standard OB, which are indeed constant triplets.
The results shows that, after linearity corrections, different methods provide evidence of a small positive shutter delay $\delta_t = +0.008 \pm 0.003$ sec.

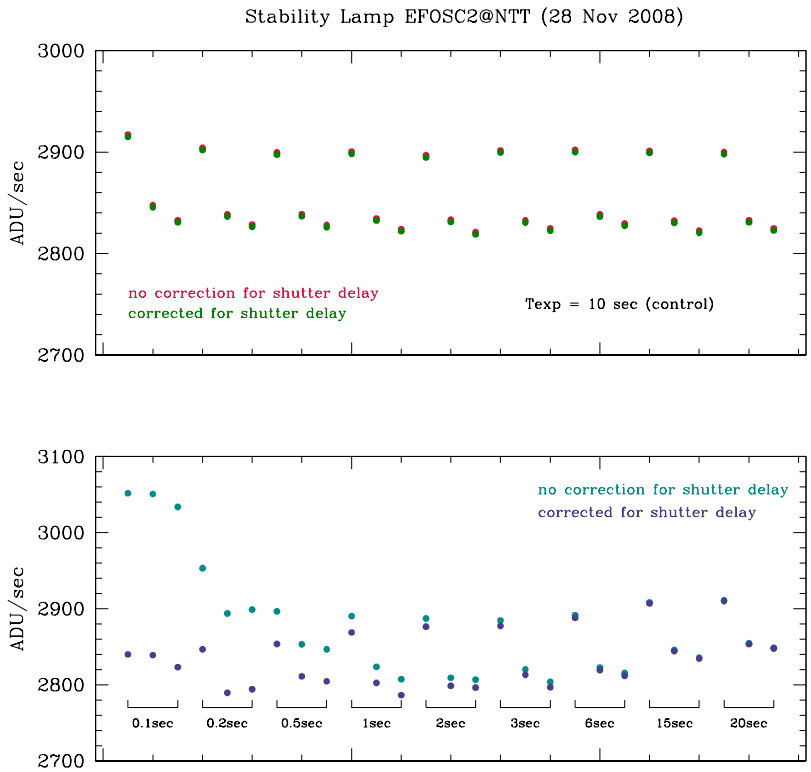

FIGURE 16: Upper panel: ADU rate for each 10 sec frame taken to monitor the lamp stability. Lower panel: ADU rate for each single frame of the shutter time test.

The flat field series can also be used to check shutter effects on the 2-D frames as explained in Section 2.3. The images in Fig. 17 show the ratio between dome flats (V band) taken on November 28, 2008 with EFOSC2@NTT in 1×1 binning mode[13]. Exposure times range from 0.1 to 20 sec for the 1×1 mode and from 0.1 to 5 sec for the 2×2 mode.
2-D shutter effects seem to be absent even for the shortest exposure times (0.1 sec). The current

[12] http://www.eso.org/sci/observing/phase2/P2PP/MANUAL/p2ppman-9.pdf
[13] Frames acquired with the 2×2 binning on November 27, 2008 give the same results, as expected, since this effect is produced by the shutter design and mechanics and not by the detector.

EFOSC2 manual[14] reports the following information: *since the shutter is of the iris type, the effective exposure time in the central region is expected to be higher than in the outer region. Nevertheless, several tests have shown than the shutter delay is* $+24ms \pm 5ms$ *across the entire CCD, with the position dependent time delay being smaller than* $10ms$*. This means that after adding* $24ms$ *to the exposure time, a maximum position dependent error of* $\pm 5ms$ *is left.* The shutter delay found by us is smaller, $\delta_t \simeq 8ms$, and no significant position dependent effect due to the iris shutter is visible also with exposure times as short as 0.1sec (a residual $5ms$ correspond to a 5% variation in the 0.1 exposure time image, that is not visible in Fig. 17).

5.2 EFOSC2 CCD linearity

Our aim is to check the linearity of the response of the CCD#40 LORAL/LESSER mounted on EFOSC2@NTT, We used the method by Stello for obtaining the linearity profile of the CCD response described in Section 3.2.

On Nov 26-27 2008 (run M-007) we obtained spectral flats using the internal lamp with the following instrumental setup: grism 3, slit 2.0 arcsec (Fig. 18). The binning of the images acquired on Nov 26 is 1×1, the binning of the images taken the day after is 2×2. Details of the acquired images are shown in Table 5. We measured the linearity for both binnings.

First we checked the lamp stability with time (we took our data in about 30 minutes, see Table 5). Fig. 19 shows the ratio between each combined collapsed image with constant exposure time and the last one. The images show that the lamp flux becomes unstable soon after the lamp is switched on, showing also colour variations with time. The second set of control images, taken about 5-10 minutes after the first, is already similar in shape to the last set of images, but with a slightly lower flux. The drift was taken into account while processing the images for the linearity test. The corrected images are analyzed according the Stello's recipe described in Section 3.2 and the results are shown in Fig. 20 and Fig. 21. Fig. 22 shows the comparison of the gain obtained using different sets of images with different exposure times for the two different binnings.

5.3 EFOSC2 Conclusions

A small positive shutter delay $\delta_t \simeq +0.008 \pm 0.001$ sec, based on the most reliable results, has been measured. It can be neglected for exposure times $t \geq 1$ sec. A 2-D shutter effect, i.e. not uniform CCD illumination, seems absent even for the shortest exposure times (0.1 sec).

The tests shows that the CCD#40 LORAL/LESSER reaches a 1.2% deviation from linearity at $\simeq 55000$ counts (it has not been possible to investigate higher intensities because the data did not reach higher values). The deviation from linearity appears starting from $\simeq 5000$ counts. The

[14] http://www.eso.org/sci/facilities/lasilla/instruments/efosc/doc/manual/EFOSC2manual_v3.2.pdf

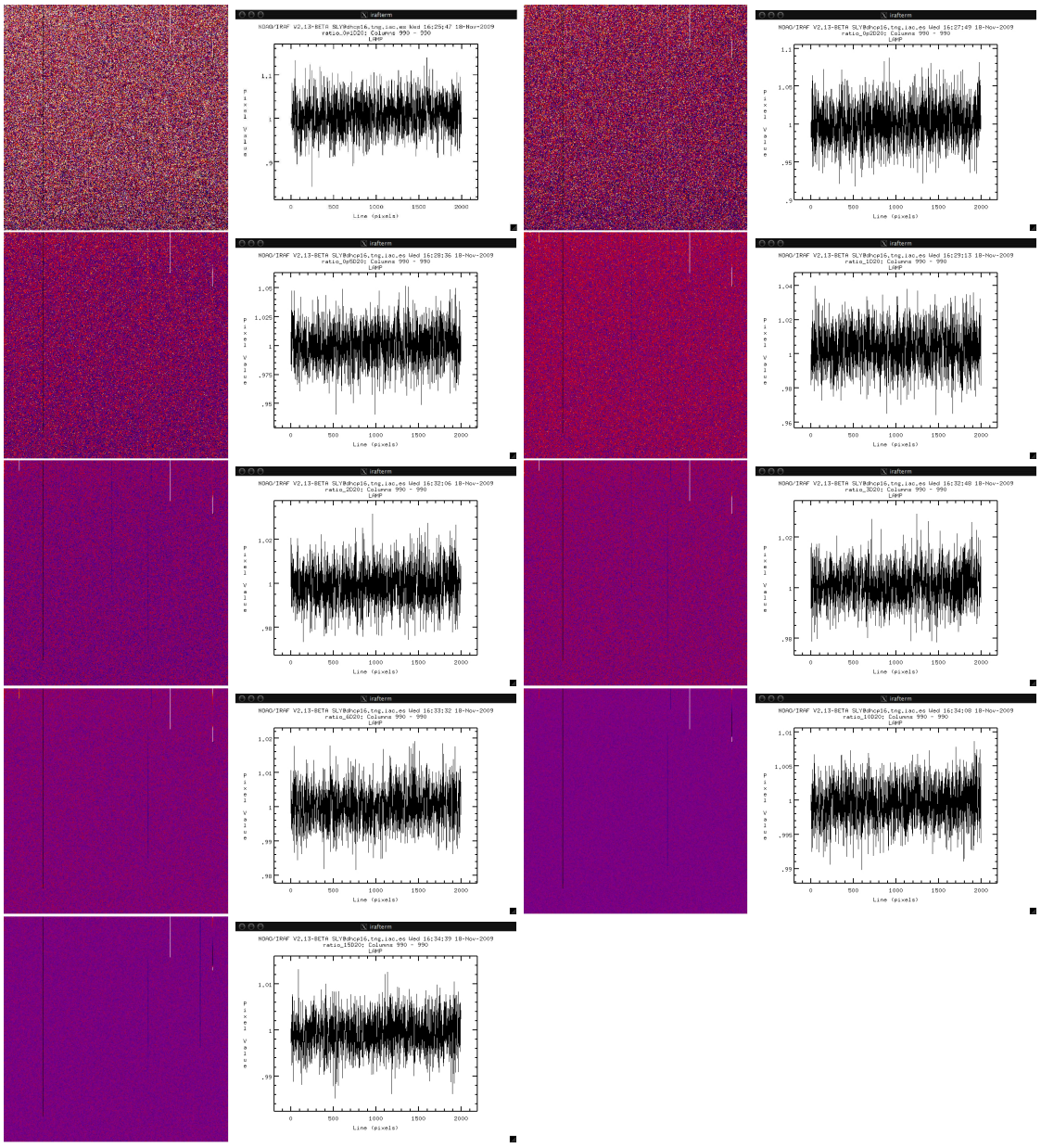

FIGURE 17: Normalized ratio of the V band masterflats with exposure time (from left to right, from the top to the bottom) equal to 0.1, 0.2, 0.5. 1, 2, 3, 6, 10 and 15 sec with respect to the 20 sec exposure. time masterflat. Colour cuts are the same for all images (z1=0.95 z2=1.05). The trace of the central column is shown on the right of each 2-D image. Data were taken on 28 Nov 2010, binning 1×1.

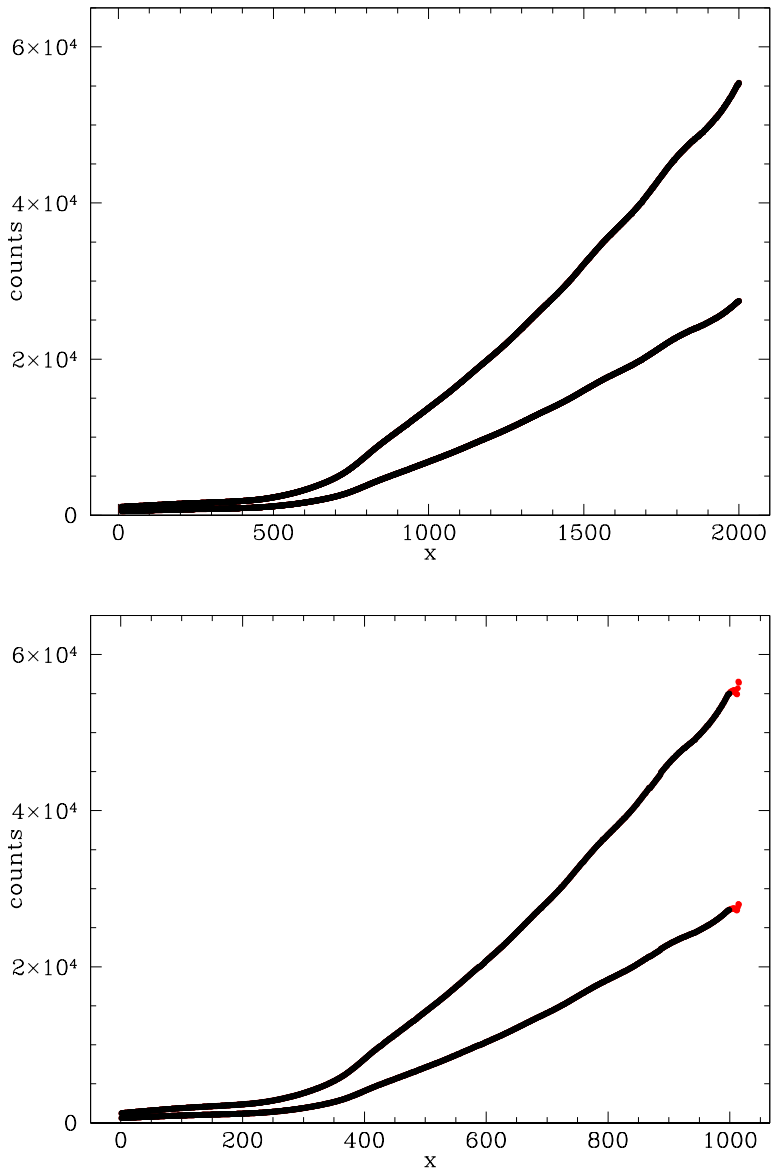

FIGURE 18: Combined spectroscopic flat field (collapsed to one-dimensional) obtained with EFOSC2@NTT using grism 3 and a 2 arcsec slit. Upper panel: exposure times of 120 and 60 sec (26 Nov 2010, binning 1×1); lower panel: exposure times of 30 and 15 sec (27 November 2010, binning 2×2).

TABLE 5: Statistics of the spectroscopic flat field (gr. 3, slit 2 arcsec) used for the linearity test at NTT

N images	BINNING	Exp. time [sec]	Counts⋆ [ADU] min	max	UT start†
		2008-11-26			
3	1x1	40	36.06	25128.	20:58:20.633
3	1x1	10	1.5	5367.	21:04:48.671
3	1x1	40	36.59	25639.	21:09:37.891
3	1x1	60	175.4	40179.	21:16:06.750
3	1x1	40	33.49	25557.	21:23:34.771
3	1x1	120	406.1	65347.	21:30:02.673
		2008-11-27			
3	2x2	10	201.	19426.	20:35:37.964
3	2x2	3	42.48	5785.	20:38:07.451
3	2x2	10	201.9	19423.	20:40:14.400
3	2x2	15	310.4	29134.	20:42:43.266
3	2x2	10	195.2	19425.	20:45:27.329
3	2x2	30	625.8	58817.	20:47:56.356
3	2x2	10	198.9	19343.	20:51:24.496

⋆ values measured on the combined image (median) of each set.
† value measured on the first image of each set.

binning does not change significantly the results: the curves obtained for the 1×1 and 2×2 binning are very similar. This results was tested correcting for linearity two spectroscopic flat fields and computing the ratio of the two flats normalized by their exposure time. Fig. 23 shows that, as expected from a correct linearity deviation correction, the ratio is flattened around 1.

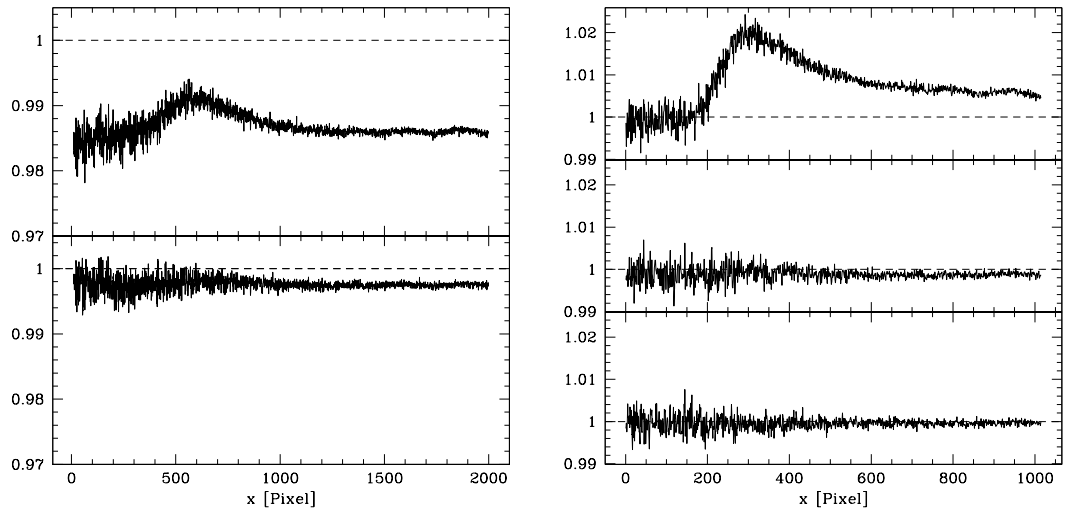

FIGURE 19: Lamp stability: each panel shows the ratio between the lamp monitoring exposures and the last one. The left image shows data taken on November 26, 2008; the right image shows the data taken on November 27, 2008.

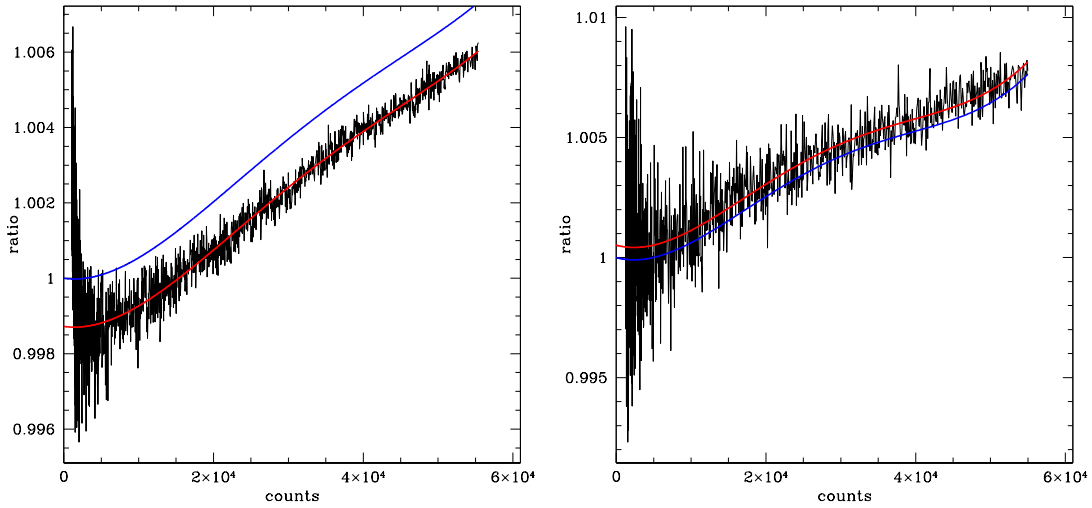

FIGURE 20: Left panel: binning 1×1, ratio $R_1 = I_{120}/120/I_{60}/60$ vs. I_{120} ; right panel: binning 2×2, ratio $R_1 = I_{30}/30/I_{15}/15$ vs. I_{15}. The 120 and 30 sec curves were corrected for possible lamp luminosity (thermal) drift (see Section 2.1). A red line shows the result after replacing the noisy curve with a polynomial fit (order 4). The curve was extrapolated to intensity zero as well. Before starting the iterative procedure, the resulting curve was multiplied by a suitable factor in order to be 1 at 0 ADU (blue curve).

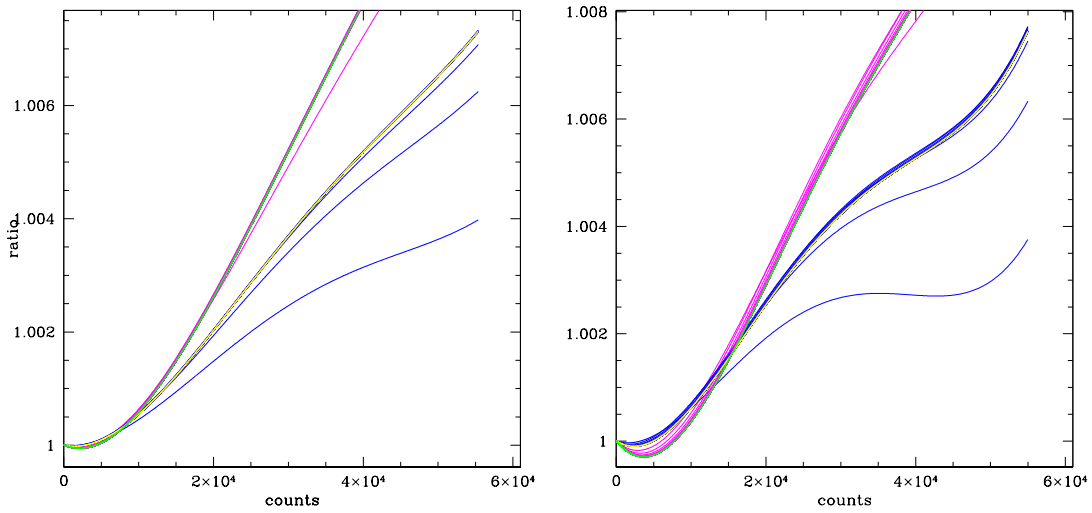

FIGURE 21: R_i iteration (blue line) converges (yellow line) on R_1 (in black but hardly seen because matched by the final iterated line) while G_i (magenta line) converges on the actual gain curve (in green). Left panel: 1×1 binning, right panel: 2×2 binning.

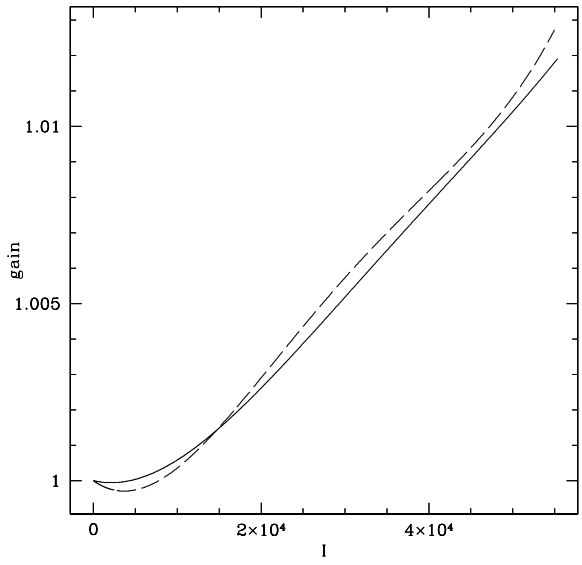

FIGURE 22: Gain curves obtained using different pairs of images for the 1×1 binning (solid line) and the 2×2 binning (dashed line).

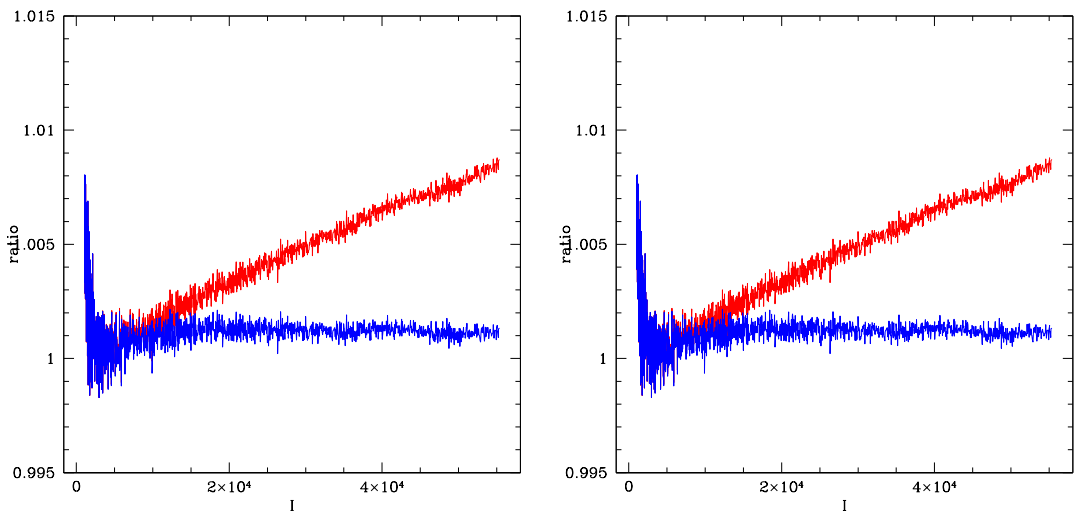

FIGURE 23: Left image: Ratio between the 120 sec and 40 sec spectroscopic flat fields before (red line) and after (blue line) linearity correction (using the correction obtained for the 1×1 binning, that made use of the 120 sec images). Right image: the same as before but with the correction obtained for binning 2×2.

6 DOLoRes@TNG 3.58m

6.1 DOLoRes Shutter effects

Our aim is to check the shutter delay of the E2V4240 CCD mounted on DOLORES@TNG[15]. We used the method described in Section 2 using data acquired to this aim by L. di Fabrizio[16] on Jan. 29, 2008. The data consist on 24 B band photometric flats, with the statistics given in Table 6.

TABLE 6: Statistics of the B flat fields used for the shutter delay test at TNG

IMAGE	MEAN [ADU]	MODE [ADU]	STDDEV [ADU]	EXPT [sec]
JQQA0055.fits	6610.	6585.	92.25	1.00
JQQA0056.fits	6603.	6595.	91.75	1.00
JQQA0057.fits	6607.	6625.	92.98	1.00
JQQA0064.fits	13271.	13221.	164.2	2.00
JQQA0065.fits	13259.	13261.	165.4	2.00
JQQA0066.fits	13249.	13266.	167.1	2.00
JQQA0073.fits	26572.	26539.	307.3	4.00
JQQA0074.fits	26536.	26638.	307.9	4.00
JQQA0075.fits	26519.	26513.	304.6	4.00
JQQA0082.fits	33221.	33235.	378.3	5.00
JQQA0083.fits	33175.	33247.	374.9	5.00
JQQA0084.fits	33157.	33170.	376.3	5.00
JQQA0091.fits	39903.	39901.	446.2	6.00
JQQA0092.fits	39846.	39727.	440.6	6.00
JQQA0093.fits	39811.	39905.	445.2	6.00
JQQA0100.fits	46469.	46479.	512.1	7.00
JQQA0101.fits	46413.	46511.	507.	7.00
JQQA0102.fits	46382.	46304.	504.2	7.00
JQQA0109.fits	53032.	52973.	568.9	8.00
JQQA0110.fits	52965.	52934.	572.5	8.00
JQQA0111.fits	52924.	52936.	567.7	8.00
JQQA0118.fits	59600.	59616.	630.8	9.00
JQQA0119.fits	59517.	59628.	629.6	9.00
JQQA0120.fits	59467.	59357.	621.7	9.00

[15]The original DOLoRes detector, a E2V4240, was replaced with a similar E2V4240 CCD in December 2007. The original CCD was used only during the pilot run P-004 in May 2007, but due to bad weather conditions, no scientific data were acquired, hence it is not necessary to characterize that CCD for our purpose.

[16]We thank L. di Fabrizio for providing us with his data and results.

The first method (Section 2.2.1) gives a shutter delay of $\delta_t = -0.006 \pm 0.002$ sec (Fig. 24). The same result is confirmed by the second method (Section 2.2.2) see Fig. 25. In both methods, data have been limited to exposure times shorter than 7 sec, i.e. intensity lower than $\simeq 40000$ ADU, because counts clearly starts to show deviation from linearity above that level (Fig. 25). If we apply a linearity correction (see Section 6.2) we can use also images with longer exposure time (i.e., higher counts) and the two methods give respectively $\delta_t = -0.013 \pm 0.003$ sec and $\delta_t = -0.010 \pm 0.001$ sec (see Fig. 24 and Fig. 25, right panel). Fig. 25 also shows that the CCD is linear within 0.5% up to 60000 ADU, as better detailed in Section 6.2.

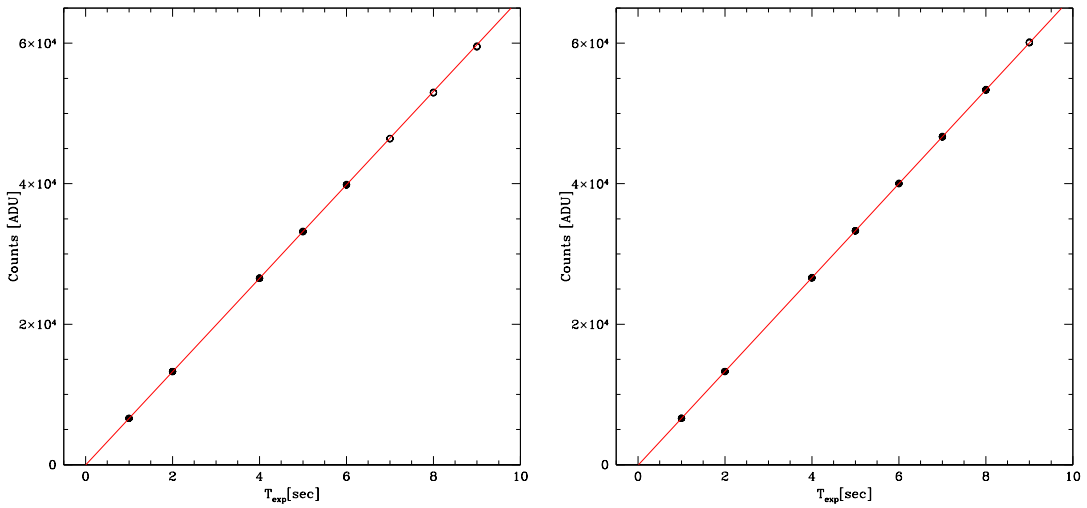

FIGURE 24: Left panel: shutter delay obtained from the data in Table 6, rejecting the points with $t \geq$ 7 sec (empty dots). The linear extrapolation to zero of the observed counts vs. exposure time crosses the time axis at $t = 0.006$ sec. The corresponding shutter delay to be summed to the exposure times is $\delta_t = -0.006 \pm 0.002$ sec. Right panel: as before but with linearity correction applied, and using all data points with $t < 9$ sec, which are slightly saturated (see Section:6.2). In this case the linear extrapolation to zero of the observed counts vs. exposure time crosses the time axis at $t = 0.013$ sec. The corresponding shutter delay is $\delta_t = -0.013 \pm 0.003$ sec.

The flat field series can also be used to check shutter effect on the 2-D frames as explained in Section: 2. The images in Fig. 26 show the ratio between dome flats (V band) taken on January 29, 2008 with DOLoRes@TNG.
The images on the right show the trend of the counts along the central column (bin 1×1). . The shutter effect seems to be absent for exposure times as short as 1 sec. Since we could not investigate shorter exposure times, we suggest to avoid exposures times shorter than 1 sec.

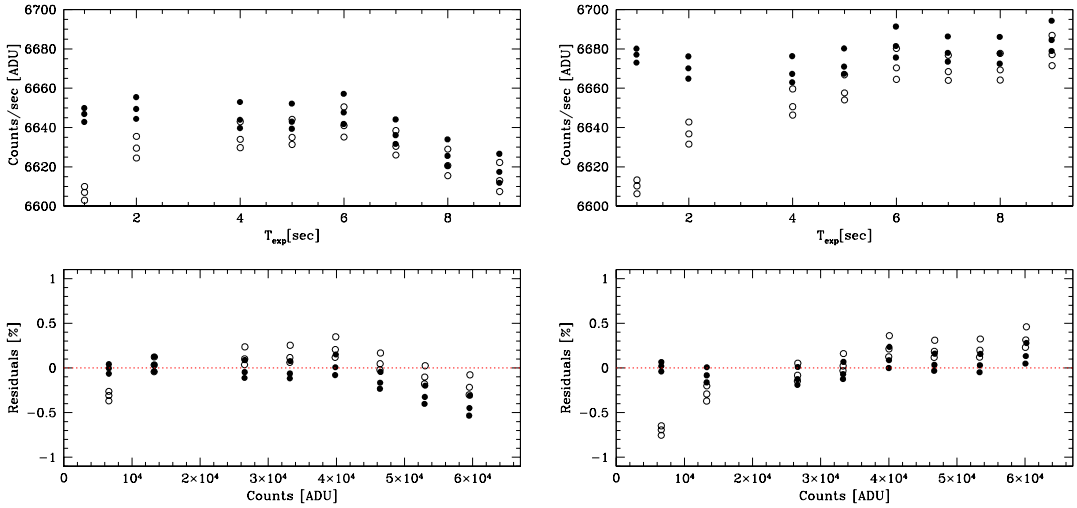

FIGURE 25: Left panels: shutter delay obtained from the data in Table 6, rejecting the points with $t \geq 7$ sec. Upper left panel: count rates vs. exposure time. Lower left panel: residual of the count rates from their average value. Empty dots are the uncorrected values; filled dots are corrected for shutter delay. The scatter from the horizontal line is minimized with $\delta_t = -0.006 \pm 0.002$ sec. The lower panel also shows that the CCD is linear within 0.5% up to 60000 ADU. Right panels: as before but with linearity correction applied and taking into account all data points with $t < 9$ sec, which are slightly saturated (see Section:6.2). The scatter from the horizontal line is minimized with $\delta_t = -0.010 \pm 0.001$ sec.

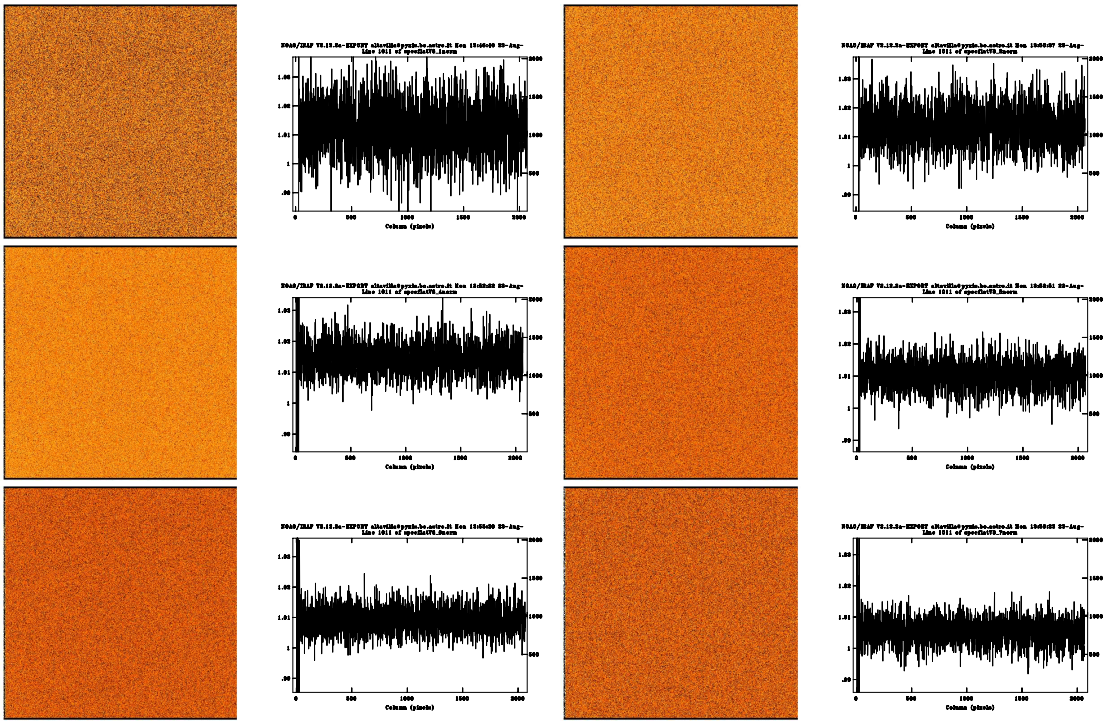

FIGURE 26: Normalized ratio between the V band masterflats with exposure times (from left to right and from the top to the bottom) equal to 1, 2, 4, 5, 6 and 7 sec with respect to the 8 sec exposure time masterflat. Colour cuts are the same for all images (z1=0.97 z2=1.02). The trace of the central line is shown on the right of each 2-D image. These frames are additional data taken on 29 Jan. 2008 by L. di Fabrizio for testing.

6.2 DOLoRes CCD linearity

Our aim is to check the linearity of the response of the E2V4240 CCD mounted on DOLORES@TNG. We used the method for obtaining the linearity profile of the CCD response described by in Section 3.2.
On Jan. 17, 2008 (run M-002) we obtained spectral flats using the internal lamp "Halogen 1" with the following instrumental setup: grism VHR-V, 2.0 arcsec slit (see Fig. 27).

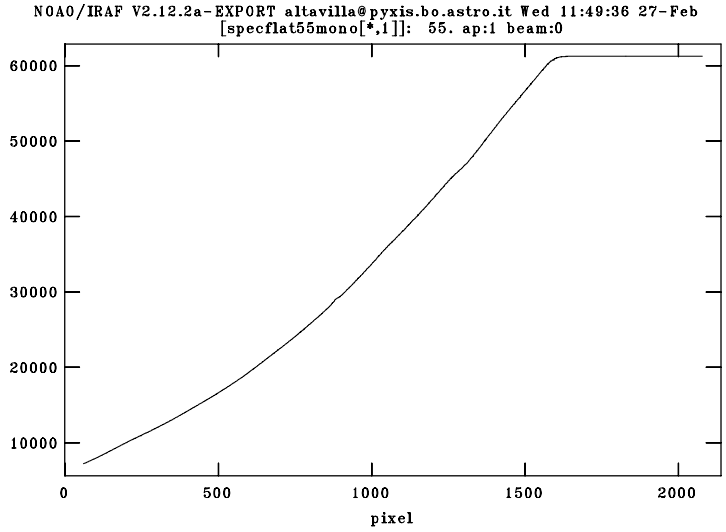

FIGURE 27: Combined spectroscopic flat field (collapsed to one-dimensional) obtained with DOLORES@TNG, grism VHR-V, 2 arcsec slit, Halogen 1 lamp and 55 sec exposure time. The saturation limit is reached on the right side of the figure.

We obtained three sets of three images each, with increasing exposure time up to saturation, spaced by sets of three images of constant exposure time to monitor the possible long term drift of the lamp. Details of the acquired images are shown in Table 7.

TABLE 7: Statistics of the spectroscopic flat fields (gr. VHR-V, slit 2 arcsec) used for the linearity test at TNG

N images	Exp. time [sec]	Counts⋆ [ADU] min	max	UT start†
3	25	3305.	37965	04:42:47
3	5	660.8	7613.	04:46:02
3	25	3290.	37821	04:48:19
3	25	3289.	37763	05:03:17
3	20	2629.	30234	05:06:34
3	25	3285.	37748	05:09:38
3	55	7222.	61231	05:12:53
3	25	3285.	37735	05:17:44

⋆ values measured on the combined image (median) of each set.
† value measured on the first image of each set.

First we checked the lamp stability along time (we took our data in about 40 minutes, see Table 7). Fig. 28 shows the ratio between each 25 sec combined spectrum and the first one. The images show that the lamp flux is not stable within the first $\simeq$ 10 minutes, but becomes more constant later on. However we noticed that the lamp does not show any colour variation with time, at least within the small VHR-V spectral range (4650–6800Å), see Fig. 28. We used the following pairs of exposure times: 55/25, 55/20 (see Fig. 29), 55/5. The corrected images are analyzed following the recipe described in Section 3.2 and the results are shown in Fig. 30. Fig. 31 shows the average gain obtained using several sets of images with different exposure times. Fig. 32 shows the comparison between our results and the results obtained by the TNG staff (provided by L. di Fabrizio, private communication). The negative trend visible at low counts in the residuals from the linear fit (Fig. 32, lower panel), may be the result of mechanical non-linearities in the shutter which are much more relevant with short exposure times rather than with long exposure times. This hypothesis was supported by the results shown in Fig. 32, when a shutter delay $t_s = -0.006$ sec[17] (see Section 6.1) was applied to get the effective exposure time. Our result shows a marginal disagreement (0.5% at most) with L. di Fabrizio's corrected results. We also point out that the data by L. di Fabrizio have not been taken in the best conditions because the lamp was switched on and off for each flat field sequence and hence never reached flux stability (from the data it seems that stability is reached $\simeq$ 10 min after switching on). In the worst case, the deviation from linearity is smaller than 1% up to saturation, at 60000 ADU.

[17]Because L. di Fabrizio's data are not corrected for linearity, we applied the t_s obtained from our data without correcting them for linearity.

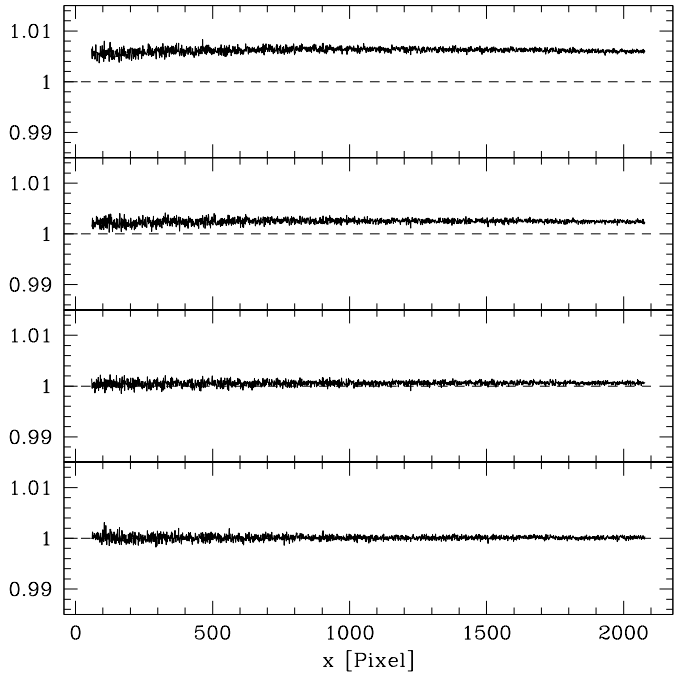

FIGURE 28: Lamp stability. Each panel shows the ratio between the control exposures (25 sec each) and the last 25 sec image.

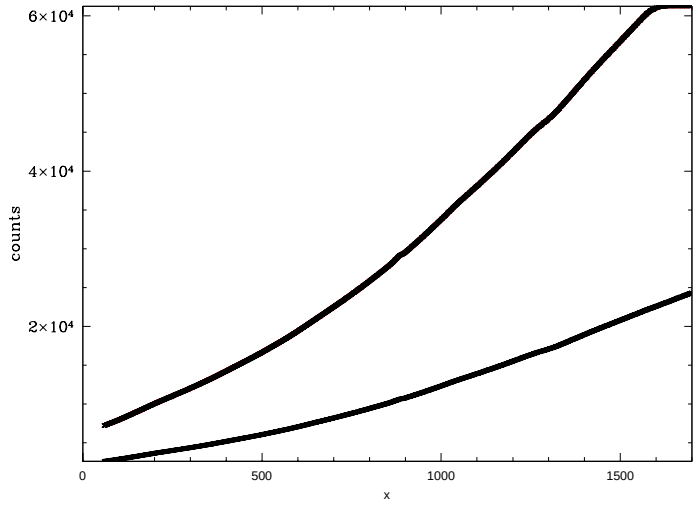

FIGURE 29: Combined spectroscopic flat field (collapsed to one-dimensional) obtained with DOLORES@TNG, grism VHR-V, slit 2 arcsec, Halogen 1 lamp, exposure time: 20 and 55 sec. Saturation limit is reached in the longest exposure time image.

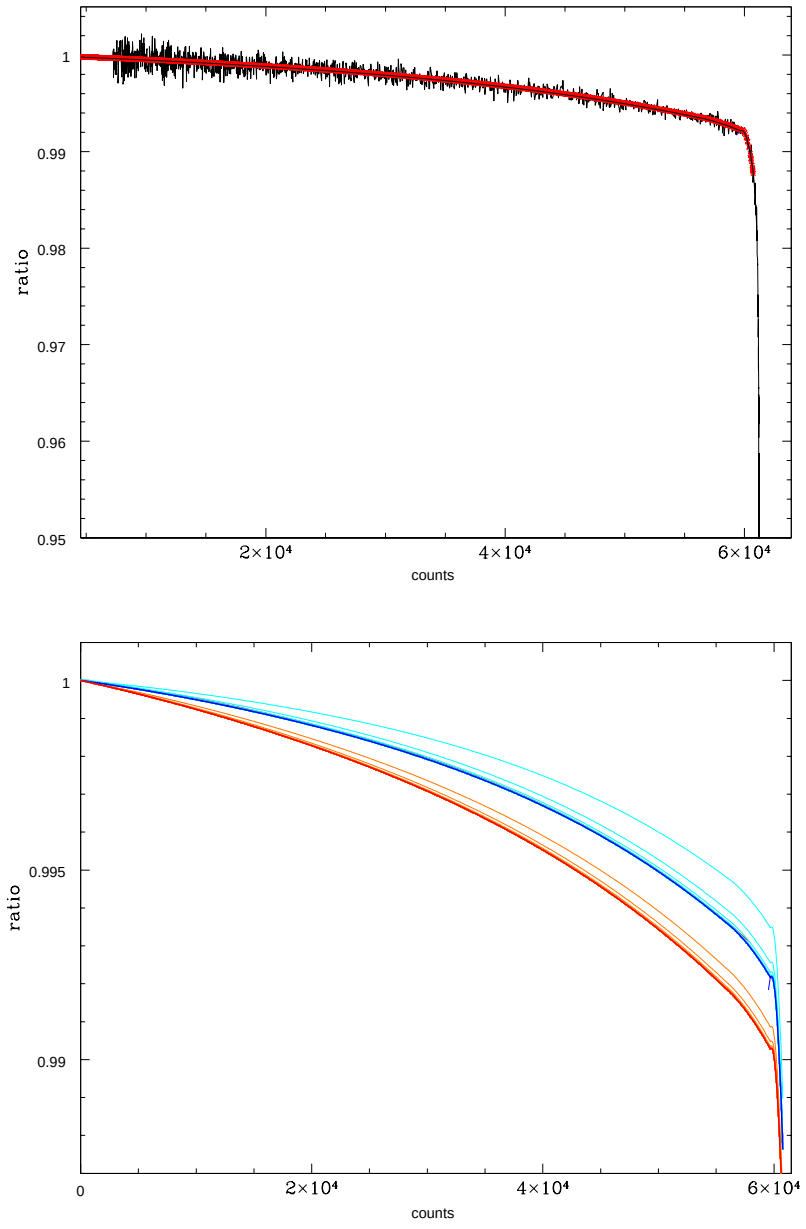

FIGURE 30: Top: Ratio $R_1 = I_{55}/55/I_{20}/20$ vs. I_{55}. The 55 sec curve has been corrected for possible lamp luminosity (thermal) drift (see Section 2.1). A red line shows the result after replacing the noisy curve with a polynomial fit (in order to get a good fit over the whole intensity range the curve was split in several sections and fitted ensuring a smooth connection of the different sections). The curve has been extrapolated to intensity zero as well. Before starting the iterative procedure, the resulting curve was multiplied by a suitable factor in order to be 1 at 0 ADU. Bottom: R_i iteration (cyan line) converges (blue line) on R_1 (in black but hardly seen because matched by the final iterated line) while G_i (orange line) converges on the actual gain curve (in red).

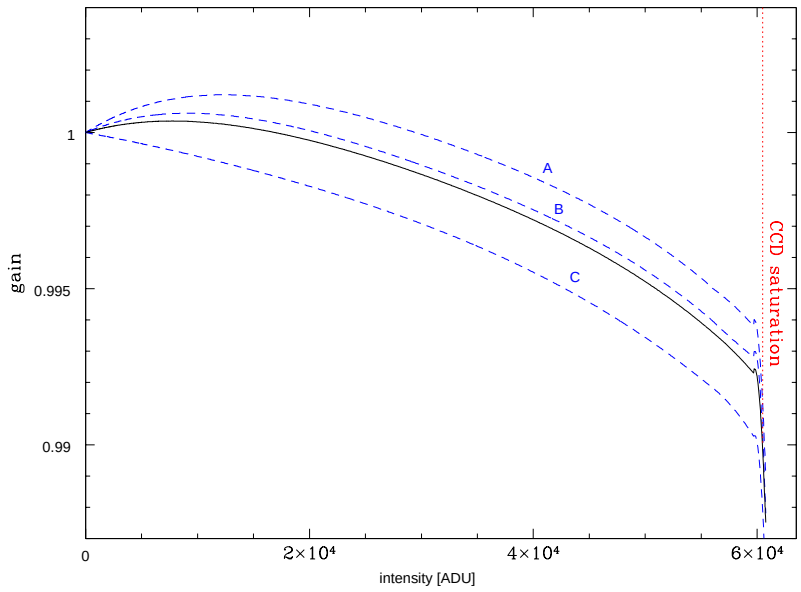

FIGURE 31: Gain curves obtained with different pairs of images and average gain (black line) obtained using four pairs of images (A and B show the ratio between the 55 sec and 5 sec curves corrected for the lamp drift computed using the control images taken before and after the 5 sec series, C shows the ratio between the 55 and 20 sec curves.

6.3 TNG Conclusions

The analysis of the TNG data shows that exposure times may be corrected by adding $t_s = -0.011 \pm 0.002$ sec (average of the various results obtained with linearity correction) to account for the shutter delay effect. 2-D shutter effect, i.e. non uniform CCD illumination, seems absent even for the shortest exposure times (1 sec). We had no data to investigate times shorter than 1 sec.

The E2V4240 CCD appears to be linear within 1% or better, up to 60000 ADU.

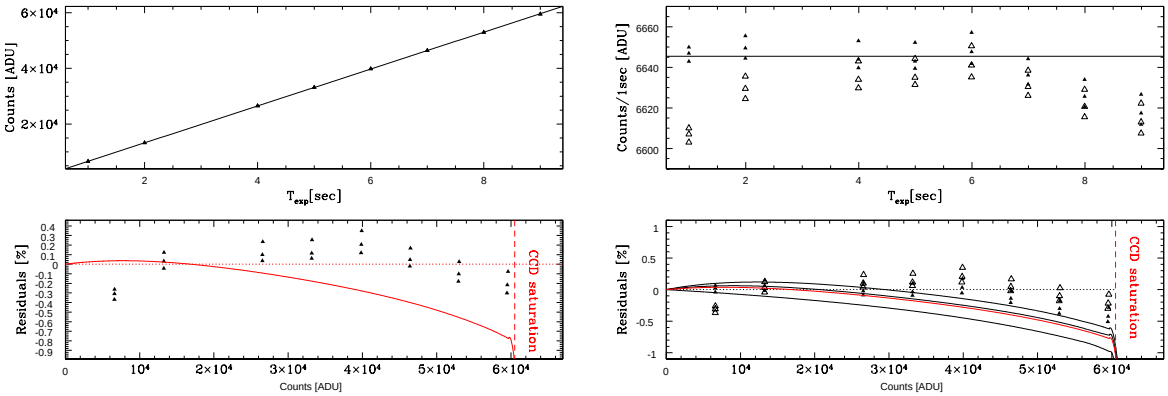

FIGURE 32: Upper left panel: linearity trend measured by L. di Fabrizio for the E2V4240 CCD. Lower left panel: comparison between the deviation from linearity measured by L. di Fabrizio (dots) and the present work (red line). Residuals were computed with respect to a linear fit which has been forced to pass through (0,0) (this assumption corresponds to zero counts for zero exposure time). Upper right panel: exposure times have been corrected with a $t_s = -0.006$ sec shutter delay correction, obtained looking for the minimum scatter around the average counts per seconds of the images with exposure times smaller than 7 sec, i.e., intensity smaller than $\simeq$ 40000 ADU, where previous tests started to show deviation from linearity. Residuals were measured with respect to a constant value given by the average counts per seconds of the images with exposure times smaller than 7 sec. The horizontal line is expected in the ideal case of a linear response over the whole dynamic range. Lower left panel: comparison between the deviation from linearity measured with the data by L. di Fabrizio, corrected for shutter delay, and the curve obtained with the Stello's method (red line, average of the four black lines). In both panels empty symbols represent the uncorrected data ($t_s = 0.0$ sec).

7 CAFOS@CAHA 2.2m

7.1 CAFOS Shutter effects

We tested the CCD SITE#1d_15 detector mounted at CAFOS for shutter effects.
In order to check the shutter time delay, we used a data set acquired on September 23, 2010 (run M-017) composed by 22 triplets of dome flat fields spanning exposure times from 0.1 to 8.7 sec. The statistics of the median combined triplets of flat fields (bias corrected and trimmed) is reported in detail in Table 8. We used two different methods to analyze the data, as described

TABLE 8: Statistics of the combined flat field (V band) used for the CAFOS shutter delay test.

IMAGE	MEAN⋆ [ADU]	MODE⋆ [ADU]	STDDEV⋆ [ADU]	Exptime [Sec]	UT start† hh:mm:ss
shuttertestV0.1_1	650.9	654.8	21.88	0.1	18:04:00
shuttertestV2_1	14433.	14576.	391.7	2.0*	18:07:41
shuttertestV0.2	1368.	1367.	41.03	0.2	18:11:14
shuttertestV2_2	14270.	14391.	387.1	2.0*	18:14:40
shuttertestV0.4	2713.	2730.	77.24	0.4	18:18:07
shuttertestV2_3	13883.	14021.	376.	2.0*	18:21:32
shuttertestV0.6	4119.	4163.	114.5	0.6	18:24:59
shuttertestV2_4	13865.	14000.	375.2	2.0*	18:28:33
shuttertestV0.8	5574.	5634.	153.1	0.8	18:32:06
shuttertestV2_5	14078.	14209.	385.5	2.0*	18:36:44
shuttertestV0.1_2	612.1	614.5	20.52	0.1	18:40:22
shuttertestV2_6	13724.	13827.	371.8	2.0*	18:43:54
shuttertestV8	55746.	56292.	1492.	8.0	18:47:20
shuttertestV2_7	13943.	14059.	375.8	2.0*	18:51:18
shuttertestV8.7	60566.	61409.	1099.	8.7	18:55:41
shuttertestV2_8	13958.	14069.	375.9	2.0*	18:59:39
shuttertestV4	28011.	28288.	752.1	4.0	19:03:06
shuttertestV2_9	13889.	14001.	374.7	2.0*	19:06:48
shuttertestV1	6937.	6989.	189.6	1.0	19:10:21
shuttertestV2_10	14039.	14198.	379.5	2.0*	19:13:44
shuttertestV6	42762.	43205.	1146.	6.0	19:17:09
shuttertestV2_11	14138.	14257.	381.	2.0*	19:20:50

* 2 sec images to monitor the lamp stability.
⋆ values measured on the combined image (median) of each set.
† value measured on the first image of each triplet.

in Section 2. The first method (Section 2.2.1) gives a shutter delay of $\delta_t = -0.023 \pm 0.005$ sec (Fig. 33). The second method (Section 2.2.2) gives $\delta_t = -0.011 \pm 0.005$ sec (Fig. 34). If we take the average we get $\delta_t = -0.017 \pm 0.007$ sec, which is less than 1% for a 2 sec exposure, hence it can be neglected for longer exposure times.

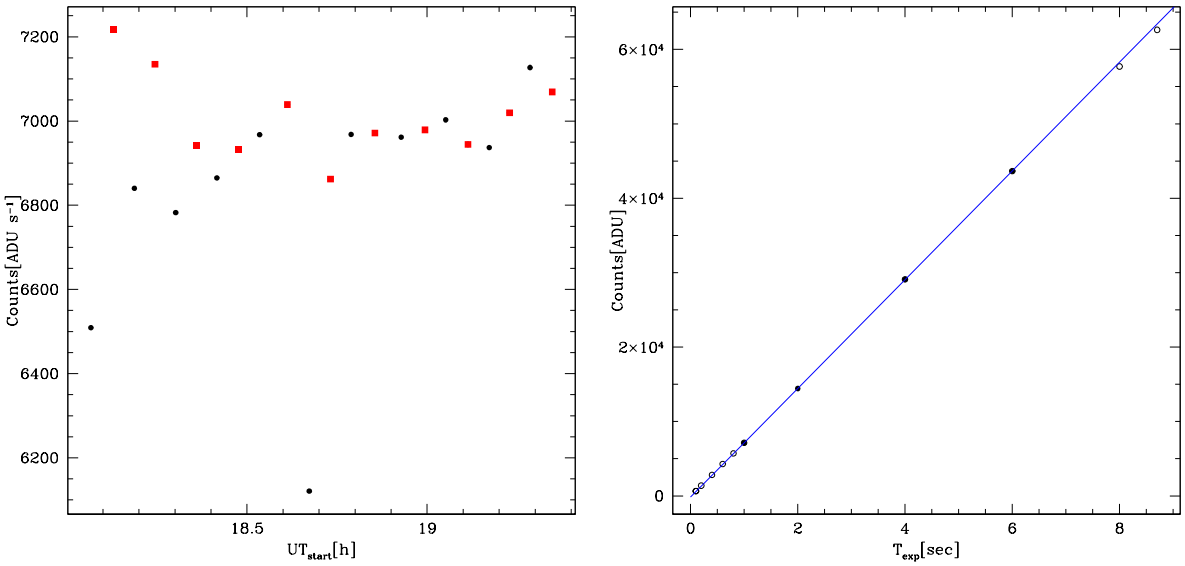

FIGURE 33: Left Panel: Counts/sec of the median combined flats per given exposure time obtained from the frames listed in Table 8. The red filled squares represent the 2 sec flats acquired to monitor the lamp (the fixed exposure time allows us to neglect possible shutter or linearity effects). Right panel: shutter delay obtained from the data in Table 8, selecting the points with $1 \leq t \leq 7$ sec (filled dots, with counts lower than 55000 ADU). Flats with the same exposure time were median combined into a single image. The linear extrapolation to zero of the observed counts (corrected for the lamp drift) vs. exposure time crosses the time axis at $t = +0.023$ sec. The corresponding shutter delay to be summed to the exposure times is $\delta_t = -0.023 \pm 0.005$ sec.

The minimum shutter time to avoid inhomogeneous illumination of the CCD was determined following the recipe described in Section 2.3 and using the data acquired on April 17, 2008 (run M-003), September 9, 2008 (run M-006), and September 23, 2010 (run M-017).

The first data set consists on 11 triplets of photometric R domeflats with exposure times of 0.1, 0.5, 1, 2, 3, 4, 5, 6, 20, 30 and 40 sec. The second data set is composed by 11 triplets of photometric R domeflats with exposure times of 0.1, 0.2, 0.5, 1, 2, 3, 4, 6, 15, 20 and 30 sec. The third data set is composed by 11 triplets of photometric unfiltered domeflats with exposure times of 0.1, 0.2, 0.4, 0.6, 0.8, 1, 2, 4, 6, 8, and 8.7 sec. The data sets produce different results, as described below.

1st Data set (April 17, 2008)
Fig. 35 clearly shows a shutter effect for exposure times shorter than $\simeq 3$ sec. With an exposure

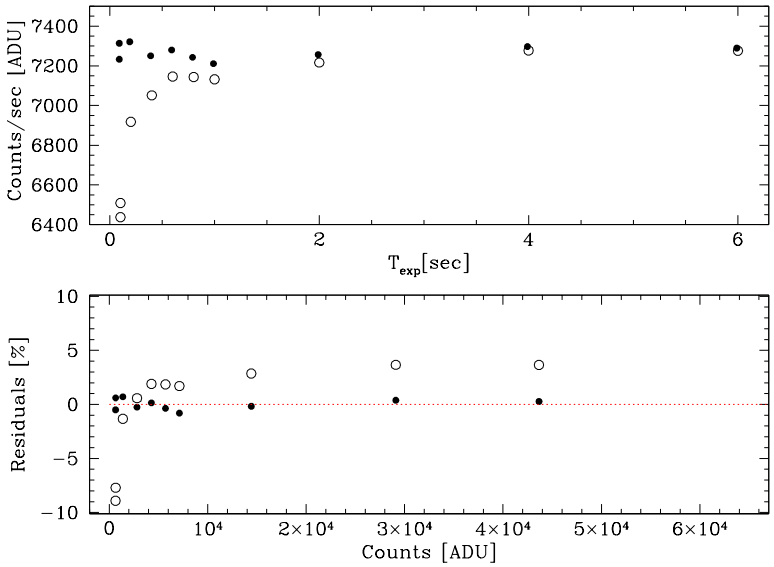

FIGURE 34: Shutter delay obtained from the data in Table 2, neglecting the points with $t > 55$ sec. Flat with the same exposure time have been median combined into a single image. Upper panel: count rates vs. exposure time. Lower panel: residual of the count rates from their average value. Empty dot are the uncorrected values; filled dots are the data corrected for shutter delay. The scatter from the horizontal line is minimized with $\delta_t = -0.011 \pm 0.005$ sec.

time of 0.1 sec there are variations of the order of about 10%. Deviations from the expected flat ratio decrease with increasing exposure time. Flat fields taken with exposure time $t_{exp} \geq 3$ sec do not show significant differences from the flat acquired with 30 sec. There is an exception for the 20 sec median combined flat. This flat was built with a series taken 1 hour before the series of 0.1–40 sec (the 20 sec flats were taken in the afternoon for the standard calibration, while the 0.1–40 sec flats were taken all together to make this test, in night-time but under bad weather). This effect hint at flat instability, nevertheless the variations are smaller than 1% (see SMR-002 for a detailed analysis of the flat stability).

2nd Data set (Sep. 9, 2008)
Fig. 36 shows that the shutter effect is now negligible, even for exposure times shorter than $\simeq 3$ sec. Weak variations (maximum amplitude $\sim 2\%$) are visible in the frames with exposure time shorter than 0.2 sec. These variations completely disappear in the frames acquired with exposure times larger than $\simeq 0.5$ sec, which do not show significant differences with respect to the flats acquired with 20 sec.

3rd Data set (Sep. 23, 2010)
The third data set (run M-017) confirms that the whole CCD is uniformly illuminated with exposure times as short as 0.6 sec (Fig. 37).

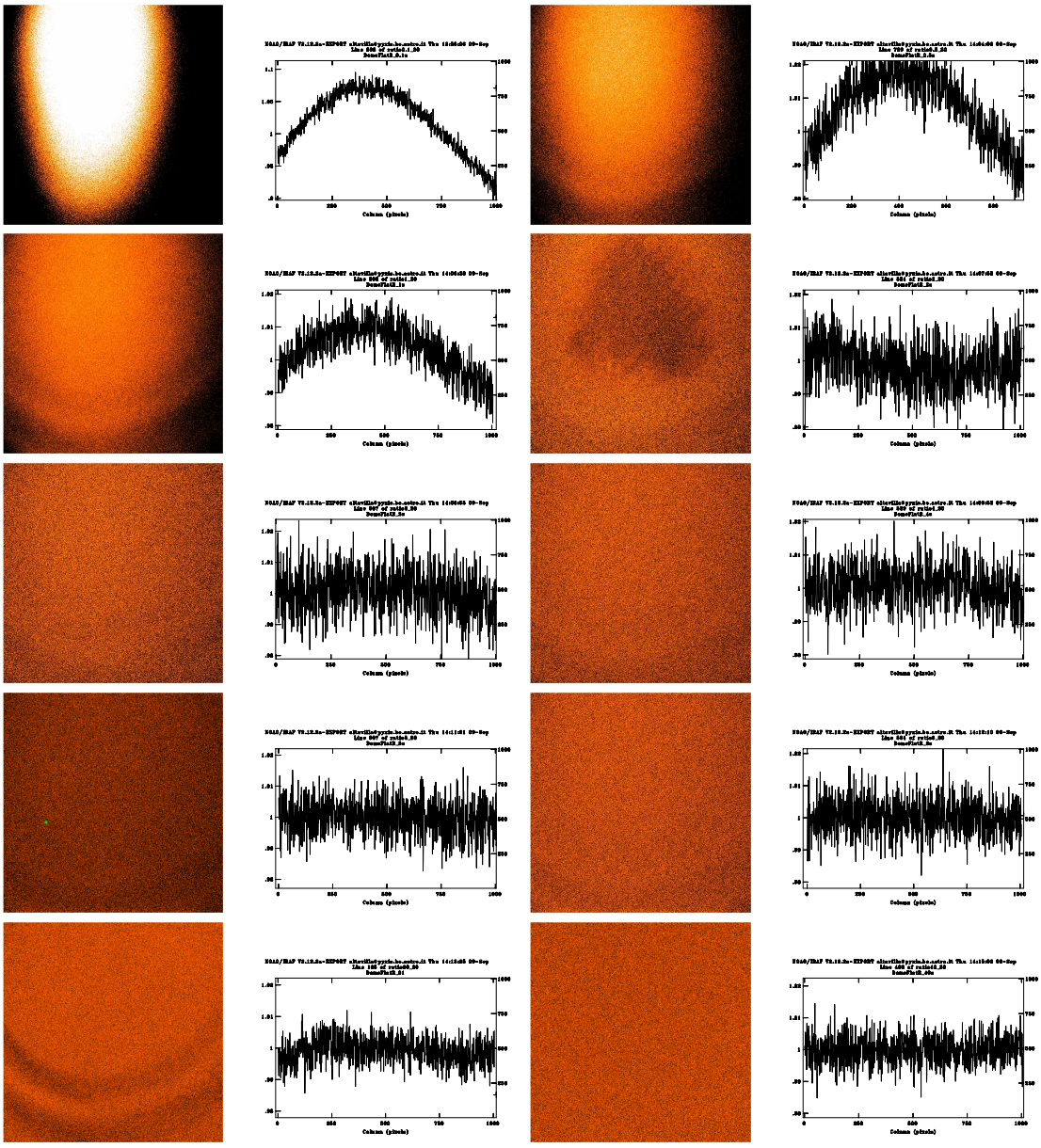

FIGURE 35: Normalized ratio between R masterflats with exposure time (from left to right, from the top to the bottom) equal to 0.1, 0.5, 1.0, 2.0, 3.0, 4.0, 5.0, 6.0, 20.0, and 40.0 sec with respect to the 30 sec exposure time masterflat. Colour cuts are the same for all images (z1=0.86 z2=1.09). The trace of the row with the biggest variation is shown on the right of each 2-D image. Data taken on April 17, 2008.

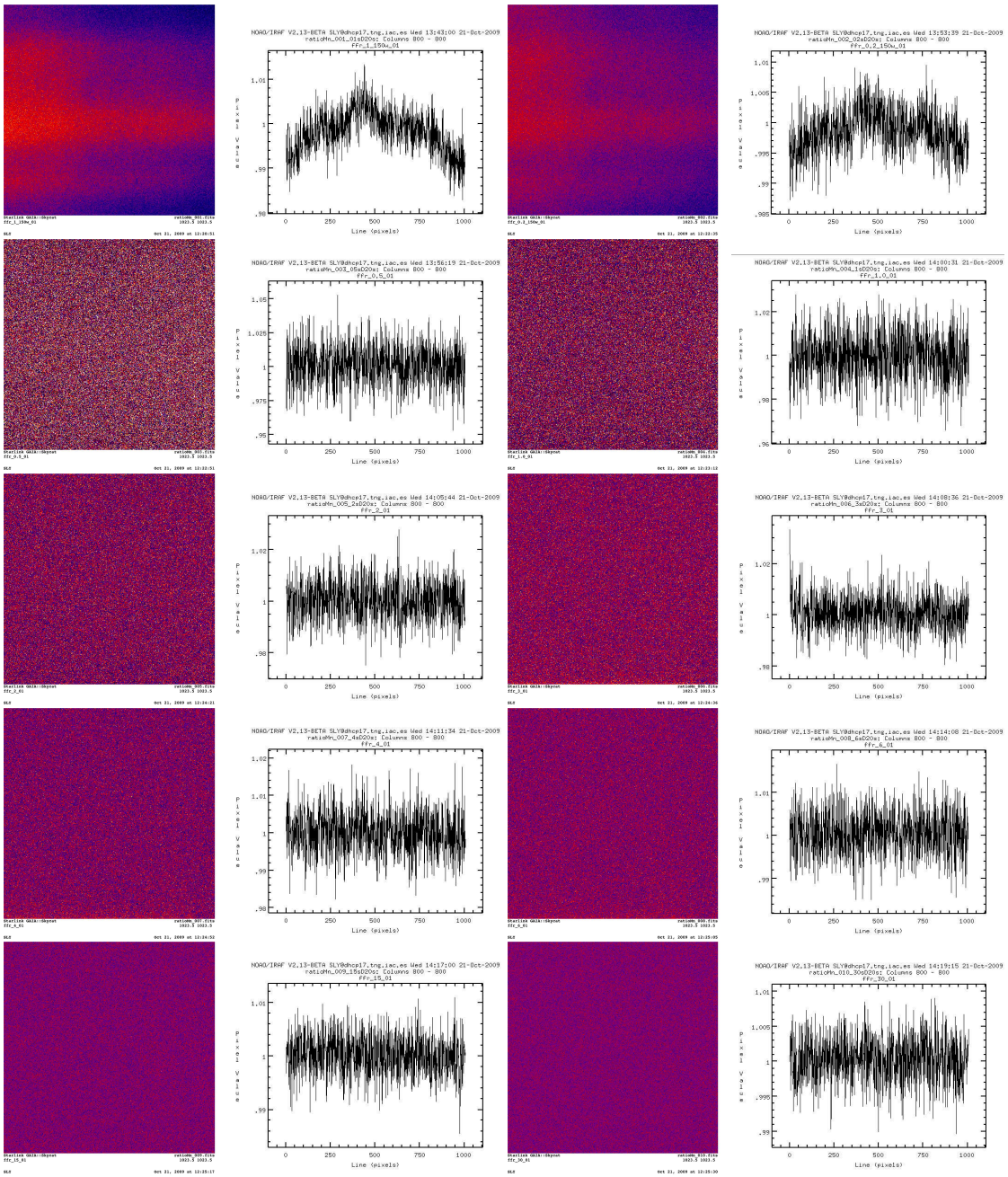

FIGURE 36: Normalized ratio between R masterflats with exposure times (from left to right, from the top to the bottom) equal to 0.1, 0.2, 0.5, 1.0, 2.0, 3.0, 4.0, 6.0, 15.0 and 30.0 sec with respect to the 20 sec exposure time masterflat. Color cuts are the same for all images (z1=0.98 z2=1.02). The trace of the row with the biggest variation is shown on the right of each 2-D image. Data taken on September 09, 2008.

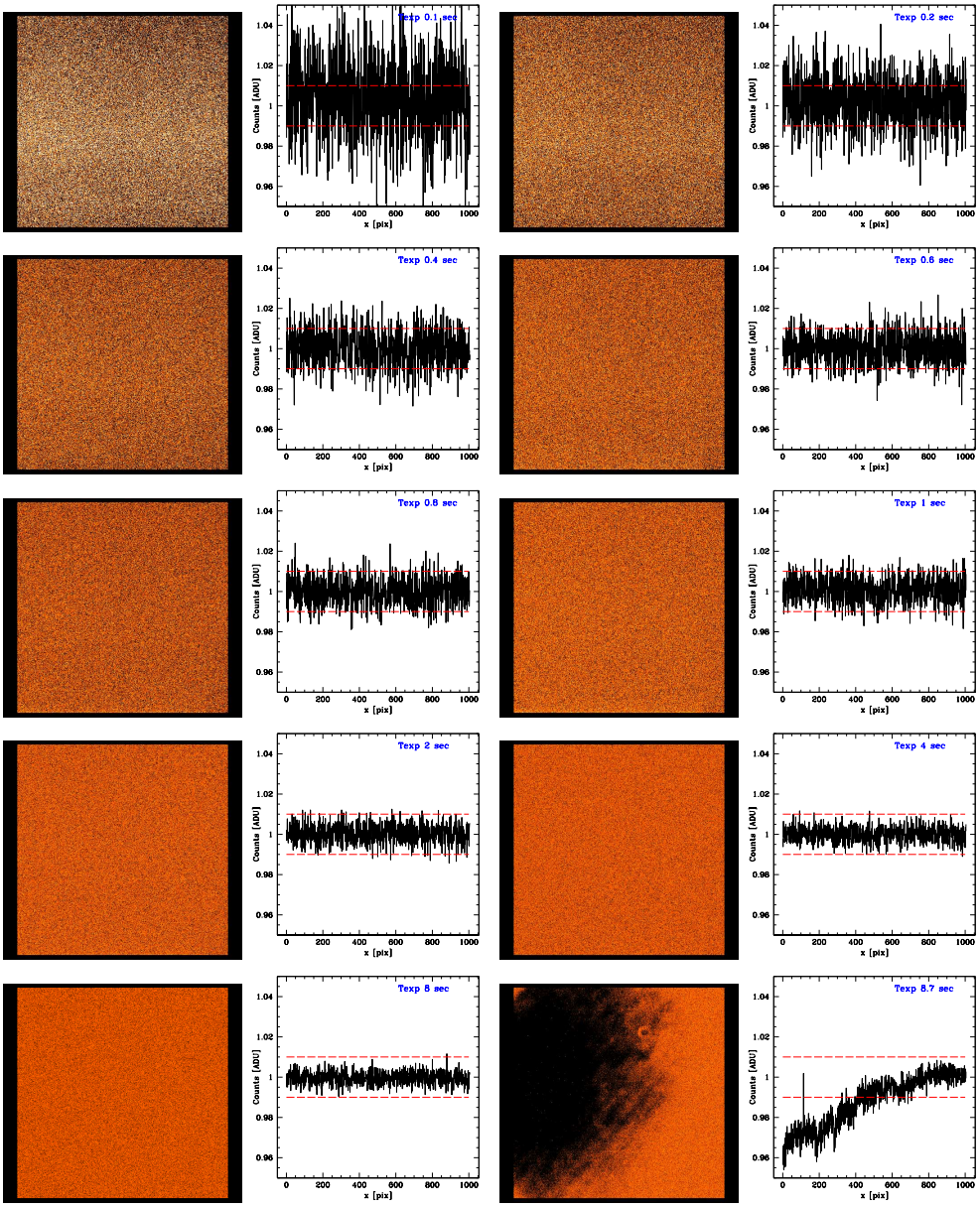

FIGURE 37: Normalized ratio between white light masterflats with exposure time (from left to right, from the top to the bottom) equal to 0.1, 0.2, 0.4, 0.6, 0.8, 1.0, 2.0, 4.0, 8.0, and 8.7 sec with respect to the 6 sec exp. time masterflat. Color cuts are the same for all images (z1=0.98 z2=1.02). The trace of the row at y=500 (the middle of the frame) is shown on the right of each 2-D image. The colour cuts are the same for all images: z1=0.98 z2=1.02. The images for the 8.7 sec frames show large deviations from linearity (the counts in the combined 8.7 sec flat vary in the range 58000-61400, so very close to saturation). This deviation is visible also in Fig. 33. Data taken on September 23, 2010.

In conclusion: the most recent data suggest that illumination inhomogeneities are negligible for exposure time $t_{exp} \geq 0.5$ sec; older data suggested the use of $t_{exp} \geq 3$ sec. The improved performance resulting from the more recent data set suggested an instrumental modification. The hypothesis that the shutter was modified/changed between the observing runs was confirmed by the CAHA staff[18]: in 2008 the old diaphragm shutter was replaced by a more efficient two blades shutter.

7.2 CAFOS CCD linearity

Our aim is to check the linearity of the response of the CCD SITE#1d_15 mounted on CAFOS@2.2m. We used the method for obtaining the linearity profile of the CCD response by Stello, described in Section 3.2.
The data to test the CCD linearity were acquired on April 1, 2007 (run P-003) with the blue grism B200 and a 2 arcsec slit width (see Fig. 38 for an example). Details of the acquired images are shown in Table 9.

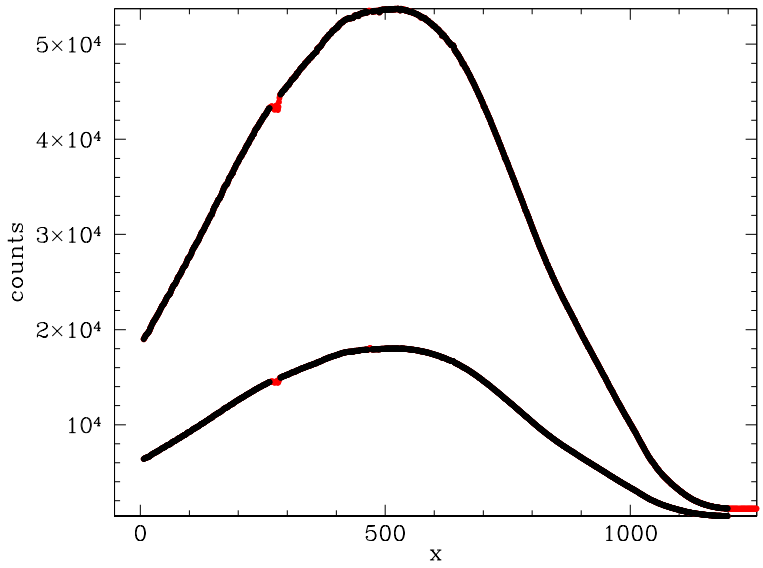

FIGURE 38: Median combined spectroscopic flat field (collapsed to one-dimensional) obtained on April 1, 2007 (run P-003) with CAFOS@2.2m, grism B200, 2 arcsec slit and exposure times of 10 and 30 sec. A small bump and the tail (marked in red) without signal were rejected.

First of all we checked the lamp stability along time (we took our data in about 1 h 40 min) as explained in Section 2.1.The images in Fig. 39 show that the lamp flux it is not perfectly stable, showing also colour variation with time. The control images taken about 1 hour from the first

[18]Santos Pedraz' private communication.

TABLE 9: Statistics of the spectroscopic flat fields (grism 3, slit 2 arcsec) used for the CAFOS linearity test

N images	BINNING	Exp. time [sec]	Counts⋆ [ADU] min	max	UT start†
3	1x1	15	529.	32594.	19:58:07
3	1x1	15*	519.	32361.	20:12:05
3	1x1	20	694.2	43200.	20:20:27
3	1x1	15*	515.2	32578.	20:27:01
3	1x1	25	886.9	61424.	20:34:31
3	1x1	15*	516.6	32854.	20:41:23
3	1x1	30	1059.	61232.	20:48:09
3	1x1	15*	517.1	32321.	21:02:42
3	1x1	5	167.6	10928.	21:09:02
3	1x1	15*	519.4	32292.	21:14:53
3	1x1	1	23.	2226.	21:22:02
3	1x1	15*	516.6	32444.	21:28:10
3	1x1	10	344.4	21914.	21:38:31

* 15 sec images to monitor the lamp stability.
⋆ values measured on the combined image (median) of each set.
† value measured on the first image of each set.

are more stable if compared to the last one.

Then the data were analyzed following the recipe by Stello described in Section 3.2 and the results are shown in Fig. 40. Fig. 41 shows, as an independent test, the ratio between the 25 sec and 10 sec spectroscopic flats (expected to be flat in the ideal case) before and after the linearity correction.

The results show that the CCD SITE#1d_15 is linear within 1% up to $\simeq 53000$ ADU and even better (within 0.1%) up to $\simeq 52000$ ADU. We do not have data to investigate the linearity at higher counts. The test is affected by the lamp luminosity drift that is so fast that the control frames taken to correct for it are not enough.

In order to check the CCD linearity at higher counts we used the classic method, described in Section 3.1, with data taken for the shutter test (see section 7.1, Table 8). Fig. 43 shows the residual of the observed points from the linear fit in Fig. 33, right panel). The plot shows that the CCD is linear within 1% up to $\simeq 55000$ ADU, thus confirming the results above. The big residuals at low counts (and short exposure times, $t_{exp} < 0.8$ sec) are due to shutter delay effects.

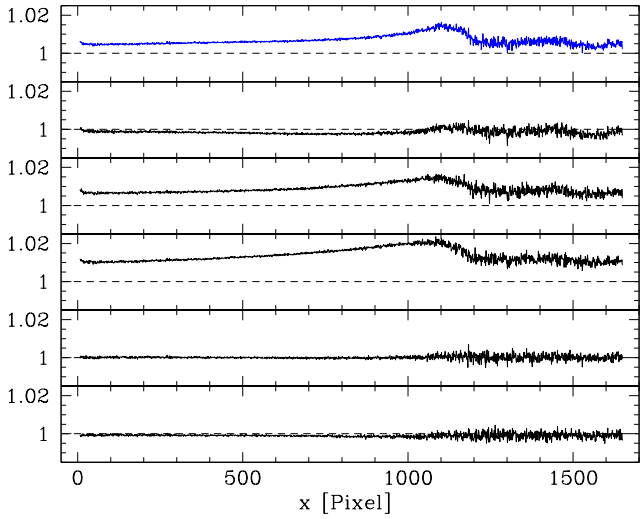

FIGURE 39: CAHA 2.2m lamp stability. Each panel shows the ratio between the control exposures (15 sec each) and the last 15 sec image (April 01, 2007), see also Table 9. The first panel is a spectroscopic flat to be used in the linearity test, but since its exposure time is 15 sec as the control frames, it can be used to monitor the lamp in the exact moment it was acquired. As better visible in Fig. 38, there is no signal after pixel $\simeq$ 1200 but just noise.

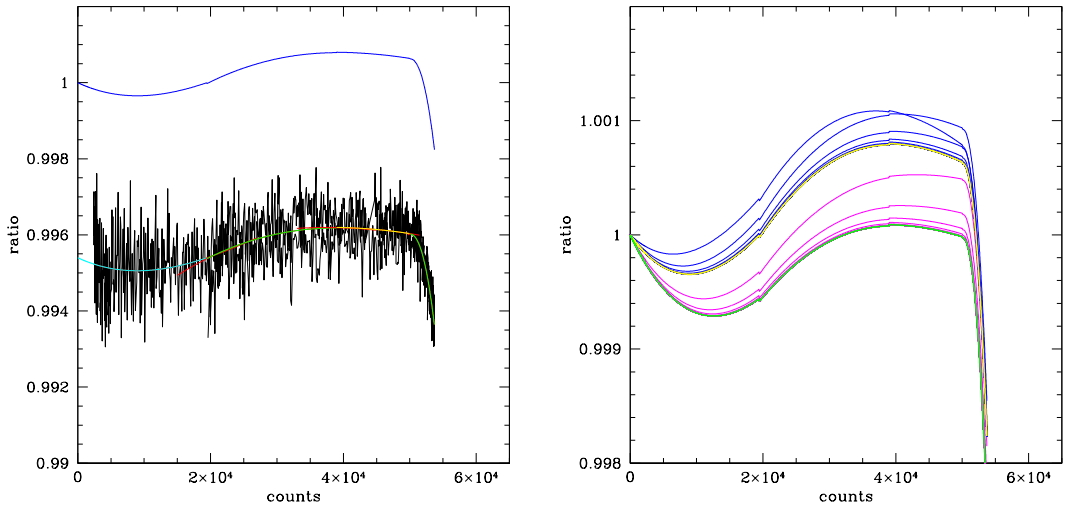

FIGURE 40: Left panel: ratio $R_1 = \frac{I_{30}/30}{I_{10}/10}$ vs. I_{30}. A coloured line shows the results after replacing the noisy curve with a polynomial fit (different colours mark the fit of different sections). The curve was extrapolated to zero intensity as well. Before starting the iterative procedure the resulting curve was scaled to be 1 at 0 ADU (blue curve). Right panel: R_i iteration (blue line) converges (yellow line) on R_1 (in black but hardly seen because matched by the final iterated line) while G_i (magenta line) converges on the actual gain curve (in green).

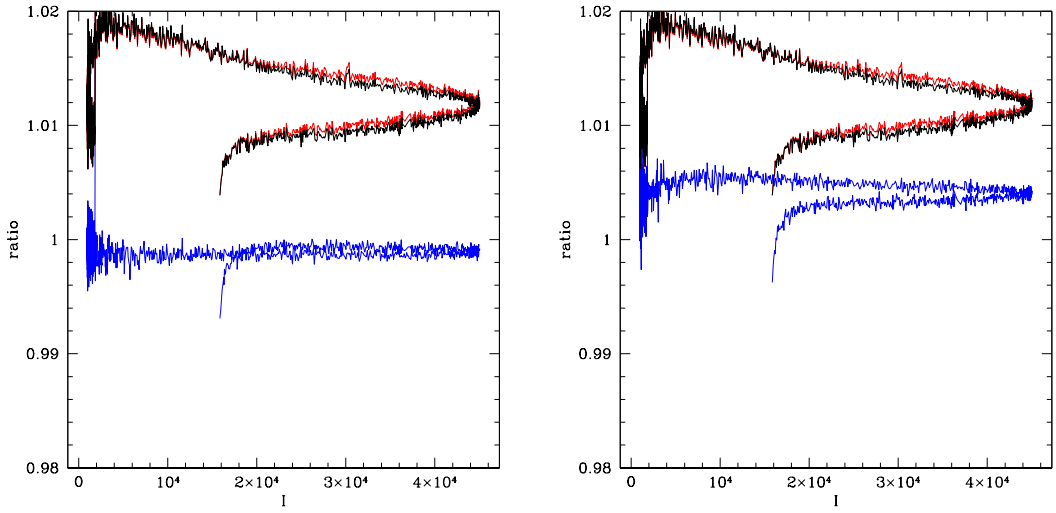

FIGURE 41: Ratio between the 25 sec and 10 sec spectroscopic flats before (red line) and after (black line) the linearity correction, and with the additional lamp drift correction (blue line). The only difference between the two panels is the lamp drift correction, built using control frames taken before (left panel) or after (right panel) the 25 sec image. Due to the fast lamp variability, the results are unstable.

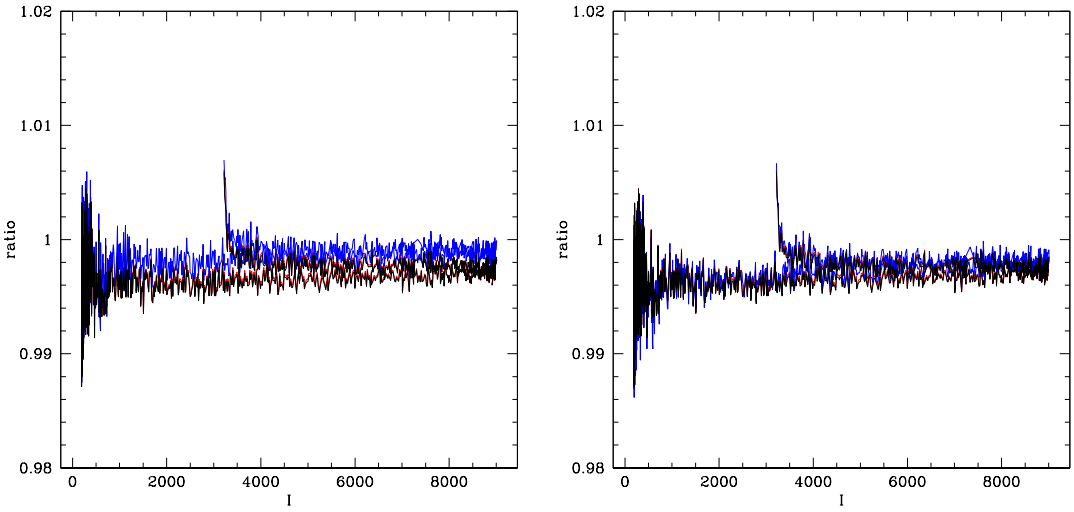

FIGURE 42: Ratio between the 10 sec and 5 sec spectroscopic flats before (red line) and after (black line) the linearity correction, and with the additional lamp drift correction (blue line). The only difference between the two panels is the lamp drift correction, built using control frames taken before (left panel) or after (right panel) the 5 sec image. These frames were acquired in the last part of our test (see Table 9) when the lamp was more stable (see Fig. 39) and in fact the correction for lamp drift is more efficient, and the results more stable if compared to Fig. 41.

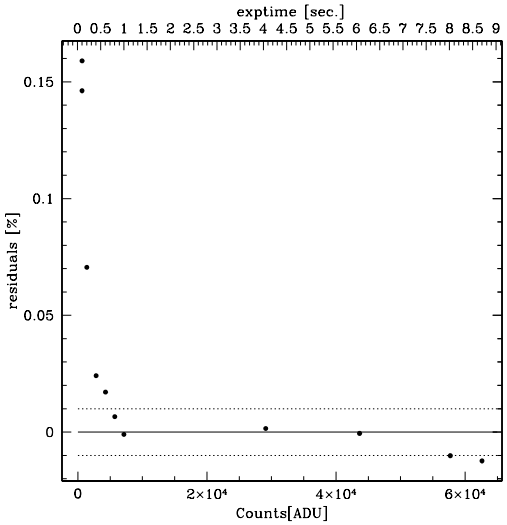

FIGURE 43: Deviation from linearity of the CCD SITE#1d_15 measured with photometric flat fields. Above $\simeq$ 55000 ADU deviation becomes larger than 1%. At lower counts (and short exposure times) the big residuals are due to shutter delay effects.

7.3 CAFOS Conclusions

A shutter delay $\delta_t = -0.017 \pm 0.07$ sec was measured with the September 23, 2010 data.

2-D shutter effect, i.e. non uniform CCD illumination, seems to be present for exposure times $t_{exp} \leq 3$ sec in images acquired in April 2008 (or before) while images taken in September 2009, with exposure times $t_{exp} \geq 0.5$ sec are homogeneously illuminated. The CAHA staff confirmed that in 2008 the old shutter was replaced with a new, faster shutter.

The tests show that the CCD SITE#1d_15 deviation from linearity is $\geq 1\%$ above $\simeq 55000$ counts. The data were not useful to explore the linearity at higher counts. Due to the lamp instability, this result is probably more pessimistic (but safer) than the real CCD characteristics.

8 ROSS@REM 0.6m

We use the REM robotic telescope only for relative photometry, therefore a detailed characterization of the shutter and CCD is less crucial than for other telescopes used in our campaigns (i.e. shutter delay and linearity effects may affect the detection of variable objects but not the absolute spectrophotometric calibration of our data). Moreover, it is not possible to obtain dome (screen) flat fields, only sky flats are automatically taken, without any control on the resulting counts. Therefore, when observing with REM, we avoid exposure times shorter than $\simeq 10$ sec and counts level higher tha 55000 ADU.

9 LaRuca@SPM 1.5m

9.1 LaRuca Shutter effects

Our aim is to test the SITE1 Photometrics CCD and the Marconi e2vm E2V-4240 CCD[19] mounted at LaRuca@1.5m for shutter effects.
Because the shutter effect is a mechanical effect, we do not expect that the results depend on the particular CCD mounted on LaRuca, also because they have a similar linear size (1072×1024 pixels corresponding to 25×25mm, and 2154×2048 pixels corresponding to 29×28mm respectively).

9.1.1 SITE1 CCD - Shutter effects

On August 23, 2008 (run V-006) we obtained photometric B dome flats for the the SITE1 Photometrics CCD. Details of the combined dome flats are shown in Table 10.

Fig. 44 shows that the lamp flux is slowly variable, with its luminosity decreasing by less than 2% in $\simeq$ 40 minutes. The data, analyzed as described in Section 2.2.1, show a shutter delay $\delta_t = +0.07 \pm 0.08$ sec, consistent with zero. see Fig. 45.

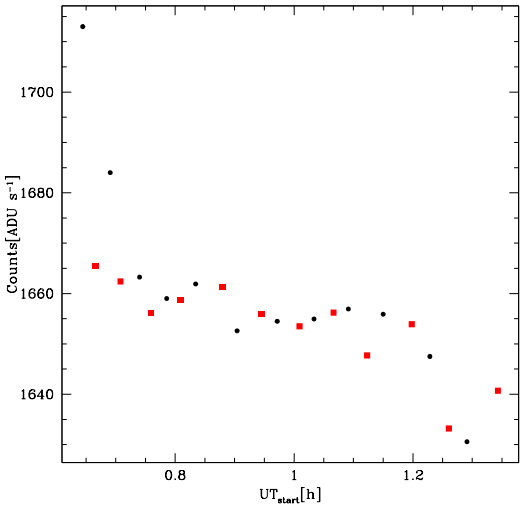

FIGURE 44: SITE1 CCD - Counts/sec of the median combined flats per given exposure time obtained from the frames listed in Table 10. The red filled squares represent the 10 sec flats acquired to monitor the lamp (the fixed exposure time allow us to neglect possible shutter or linearity effects). It is evident that the flux variation is quite slow. This fact allow us to perform a good correction of the other frames using the monitoring frames to scale properly the images.

[19]The SITE1 was the CCD in use before October 2009, when it was replaced by the new Marconi CCD.

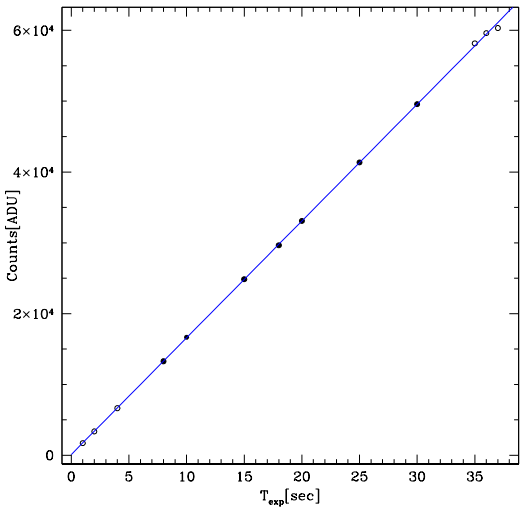

FIGURE 45: SITE1 CCD - flats with the same exposure time were median combined into a single image (see Table 10). The linear extrapolation to zero of the observed counts vs. exposure time crosses the time axis at $t = -0.07$ sec. The fit is based on the points already corrected for the lamp drift, with $5 < t \leq 30$ sec, and counts lower than 55000 ADU (filled dots) to avoid saturation effects. The corresponding shutter delay is $\delta_t = +0.07 \pm 0.08$ sec.

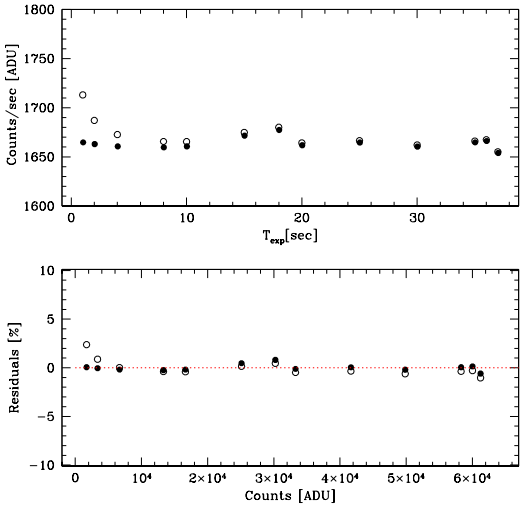

FIGURE 46: SITE1 CCD - Shutter delay obtained from the data in Table 10, rejecting points with $t > 30$ sec in the fit. Upper Panel: counts rate vs. exposure time. Lower panel: residuals of the count rates from their average value. Empty dots are the uncorrected values; filled dots are corrected for shutter delay. The scatter from the horizontal line is minimized with $\delta_t = +0.029 \pm 0.003$ sec. The same plot shows that the CCD linear within 1% also above 60000 counts, with deviations from linearity probably starting very close to saturation.

TABLE 10: Statistics of the photometric flat field used for the linearity test at San Pedro Mártir - SITE1 CCD

Name	Mean⋆	Min.⋆	Max.⋆	Exp. time	UT start†
SPMshuttertestB1	1713.	251.7	1926.	1.0	00:38:40
SPMshuttertestB10_1	16655.	2054.	18593.	10.0	00:39:56
SPMshuttertestB2	3368.	428.8	3784.	2.0	00:41:26
SPMshuttertestB10_2	16624.	2075.	18633.	10.0	00:42:28
SPMshuttertestB4	6653.	848.9	7456.	4.0	00:44:24
SPMshuttertestB10_3	16561.	2072.	18473.	10.0	00:45:36
SPMshuttertestB8	13272.	1679.	14828.	8.0	00:47:08
SPMshuttertestB10_4	16588.	2080.	18715.	10.0	00:48:32
SPMshuttertestB35	58166.	7143.	64765.	35.0	00:50:04
SPMshuttertestB10_5	16613.	2030.	18561.	10.0	00:52:47
SPMshuttertestB30	49578.	6120.	55580.	30.0	00:54:15
SPMshuttertestB10_6	16560.	2051.	18398.	10.0	00:56:43
SPMshuttertestB25	41362.	5044.	45995.	25.0	00:58:18
SPMshuttertestB10_7	16535.	2036.	18454.	10.0	01:00:33
SPMshuttertestB20	33099.	4112.	37129.	20.0	01:02:01
SPMshuttertestB10_8	16562.	2066.	18548.	10.0	01:03:59
SPMshuttertestB15	24854.	3103.	27695.	15.0	01:05:29
SPMshuttertestB10_9	16477.	2057.	18297.	10.0	01:07:23
SPMshuttertestB36	59612.	7336.	64999.	36.0	01:09:00
SPMshuttertestB10_10	16539.	2039.	18497.	10.0	01:11:53
SPMshuttertestB18	29655.	3678.	33161.	18.0	01:13:43
SPMshuttertestB10_11	16332.	1992.	18236.	10.0	01:15:38
SPMshuttertestB37	60331.	7461.	64818.	37.0	01:17:28
SPMshuttertestB10_12	16407.	2020.	18333.	10.0	01:20:35

⋆ values measured on the combined image (median) of each set.
† value measured on the first image of each set.

We also tried to check the shutter delay with the second method, described in Section 2.2.2. In this case $\delta_t = +0.029 \pm 0.003$ sec, see Fig. 46. In both methods, data have been limited to exposure times shorter than 30 sec, i.e., intensity lower than $\simeq 55000$ ADU, to avoid significant strong deviation from linearity effects.

We used the method described in Section 2.3 to check for the minimum exposure time to avoid an inhomogeneous illumination of the CCD. The images in Fig. 47 are based on white light dome flats taken on August 20, 2008 with LaRuca@1.5m equipped with the SITE1 CCD (run V-006). Exposure times go from 0.1 to 20 sec.

A iris shutter effect is clearly visible for exposure times shorter than $\simeq 10$ sec, even if the effect is quite small for exposure times ≥ 4sec. With an exposure time of 0.1 sec there are variations of the order of about 6%. Deviations decrease while increasing the exposure time: $\simeq 4$ sec flats show differences of about 1% from the flat acquired with 20 sec, and 10 sec flats are more homogeneous also at the corners where the other images show a bigger deviations.

Fig. 48 shows the ratio between two flat fields taken with the same exposure time (1 sec) but with different a lamps setup. This test was done to check for possible dependencies of the CCD illumination from the used lamp, in fact a faint lamp was used for exposure times longer than 1 sec and a bright one for exposure times shorter than 1 sec. The frames with the longest exposure time (10 and 20 sec), were acquired with the flat field lamps off, the standard dome illumination was enough.

As expected the ratio between the 1 sec exposures taken with different lamps is quite flat, but some black/white shadows (also visible in Fig. 47) suggest that some dust grain moved inside the optics. This effect is especially visible in Fig. 49 which shows the appearing of a dust shadow during a consecutive flat field sequence. If the same happens during a sequence on a target, the flat field correction would produce a sudden *jump* in the photometric measurements.

The results suggest to avoid exposure times shorter than $\simeq 5$ sec.

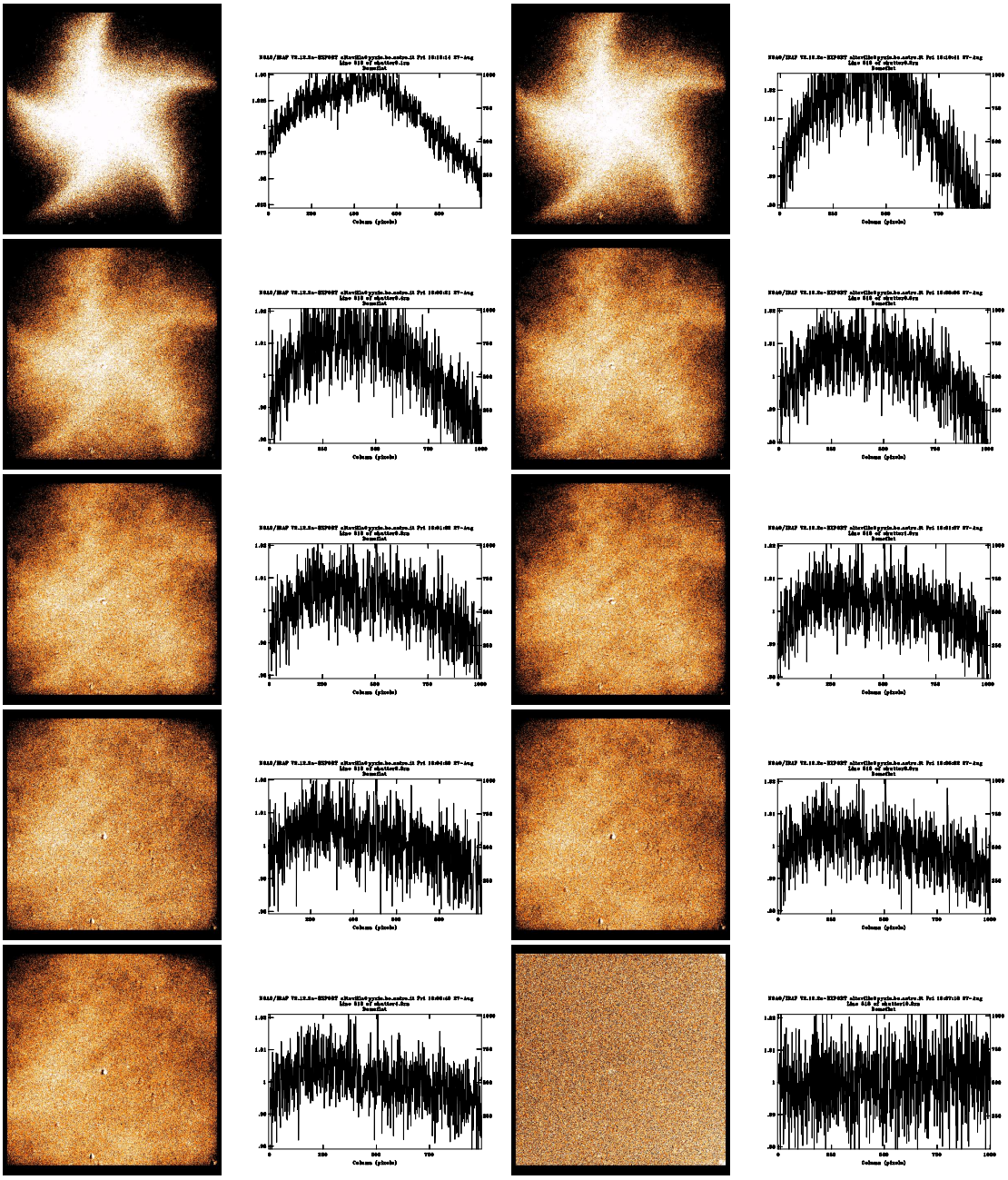

FIGURE 47: SITE1 CCD - Normalized ratio between white light masterflats with exposure time, from left to right, from the top to the bottom, equal to 0.1, 0.2, 0.4, 0.6, 0.8, 1.0, 2.0, 3.0, 4.0, 10.0 sec and the 20 sec exposure time masterflat. The iris structure is clearly visible with very short exposure times. The trend of the counts along a central row of each image is shown too. Colour cuts are the same for all images (z1=0.99 z2=1.01). Data were taken on August 20, 2008.

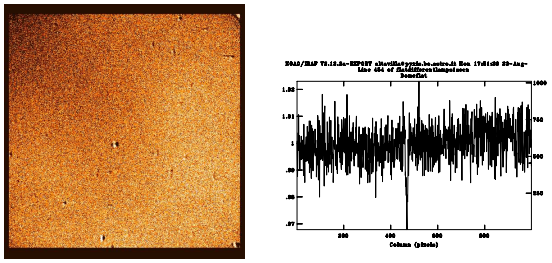

FIGURE 48: Normalized ratio between white light masterflats with 1 sec exposure time but different lamps setups. Colour cuts are z1=0.99 z2=1.01. The data were taken on August 20 2008.

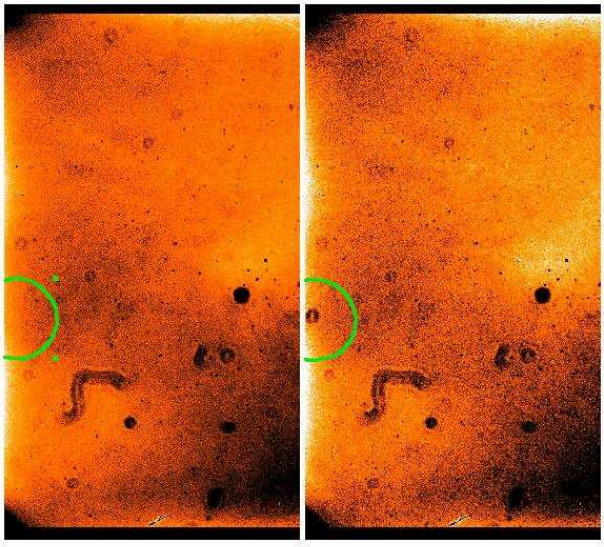

FIGURE 49: Comparison between V flat fields taken on August 19, 2008. A dust shadow appeared suddenly within the same consecutive flat field sequence (its position is marked by a green circle in the images).

9.1.2 MARCONI CCD - Shutter effects

On July 17, 2010 (run V-020) we obtained photometric dome flats for the Marconi e2vm E2V-4240 CCD. Details of the combined dome flats are shown in Table 11.

TABLE 11: Statistics of the photometric flat field used for the linearity test at San Pedro Mártir - Marconi CCD

Name	MODE⋆	Min.⋆	Max.⋆	Exp. time	UT start†
SPMlinearitytestR20_1.fits	14304.	792.5	23549.	20.0	06:19:57
SPMlinearitytestR2.fits	1451.	96.53	2410.	2.0	06:22:22
SPMlinearitytestR20_2.fits	14326.	785.	23606.	20.0	06:23:52
SPMlinearitytestR4.fits	2877.	164.6	4742.	4.0	06:26:27
SPMlinearitytestR20_3.fits	14378.	776.4	23641.	20.0	06:28:00
SPMlinearitytestR7.fits	5058.	283.1	8367.	7.0	06:30:50
SPMlinearitytestR20_4.fits	14449.	792.9	23781.	20.0	06:32:36
SPMlinearitytestR14.fits	10099.	547.1	16597.	14.0	06:34:59
SPMlinearitytestR20_5.fits	14373.	781.2	23577.	20.0	06:37:03
SPMlinearitytestR28.fits	19910.	1098.	32749.	28.0	06:39:24
SPMlinearitytestR20_6.fits	14393.	780.5	23586.	20.0	06:42:49
SPMlinearitytestR40.fits	28800.	1577.	47271.	40.0	06:45:19
SPMlinearitytestR20_7.fits	14384.	790.8	23765.	20.0	06:49:14
SPMlinearitytestR56.fits	40315.	2197.	62929.	56.0	06:52:06
SPMlinearitytestR20_8.fits	14377.	783.2	23759.	20.0	06:58:34
SPMlinearitytestR62.fits	44624.	2468.	62925.	62.0	07:00:58
SPMlinearitytestR20_9.fits	14347.	812.4	23645.	20.0	07:05:21
SPMlinearitytestR68.fits	48742.	2648.	62950.	68.0	07:07:41
SPMlinearitytestR20_10.fits	14353.	776.7	23706.	20.0	07:13:27
SPMlinearitytestR74.fits	53025.	2900.	62890.	74.0	07:16:04
SPMlinearitytestR20_11.fits	14240.	789.6	23435.	20.0	07:21:07
SPMlinearitytestR80.fits	57460.	3162.	62947.	80.0	07:24:05
SPMlinearitytestR20_12.fits	14361.	793.2	23657.	20.0	07:29:56
SPMlinearitytestR87.fits	62917.	3409.	62963.	87.0	07:32:17
SPMlinearitytestR20_13.fits	14339.	830.6	23534.	20.0	07:38:46
SPMlinearitytestR89.fits	62947.	3494.	62963.	89.0	07:41:11
SPMlinearitytestR20_14.fits	14309.	796.5	23608.	20.0	07:47:10

⋆ values measured on the combined image (median) of each set.
† value measured on the first image of each set.

Fig. 50 shows that the lamp flux it is quite stable stable, with its luminosity decreasing by less

than 2% in $\simeq$ 90 minutes. Fig. 51 shows that the Marconi CCD is affected by a small shutter delay $\delta_t = -0.06 \pm 0.15$ sec, compatible with zero within the uncertainties.

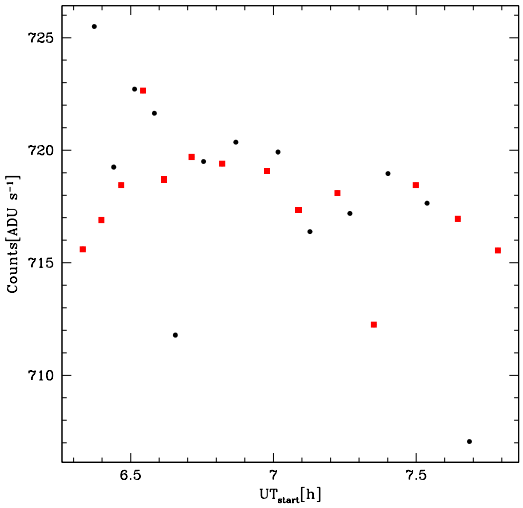

FIGURE 50: Marconi CCD - Counts/sec of the median combined flats per given exposure time obtained from the frames listed in Table 11. The red filled squares represent the 20 sec flats acquired to monitor the lamp (the fixed exposure time allow us to neglect possible shutter or linearity effects). It is evident that the lamp is quite stable.

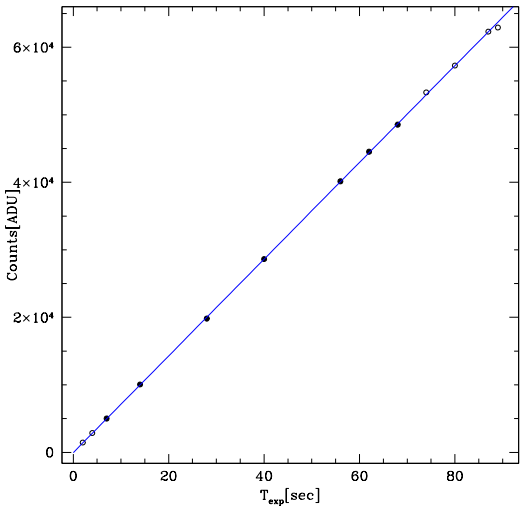

FIGURE 51: Marconi CCD - flat fields with the same exposure time were median combined into a single image (see Table 11). The linear extrapolation to zero of the observed counts vs. exposure time crosses the time axis at $t = 0.06$ sec. The fit is based on the points already corrected for lamp drift and with $5 < t \leq 70$ sec, and counts lower than 50000 ADU (filled dots) to avoid saturation effects. The corresponding shutter delay is $\delta_t = -0.06 \pm 0.15$ sec.

We also tried to check the shutter delay with the second method (Section 2.2.2), see Fig. 52. In

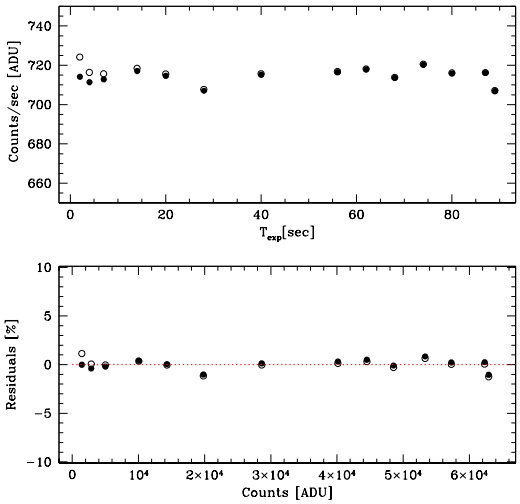

FIGURE 52: Marconi CCD - Shutter delay obtained from the data in Table 11, rejecting the points with $t > 70$ sec. Upper Panel: count rates vs. exposure time. Lower panel: residuals of the count rates from their average value. Empty dots are the uncorrected values; filled dots are corrected for shutter delay. The scatter from the horizontal line is minimized with $\delta_t = +0.028 \pm 0.004$ sec. The same plot show that the CCD linear within 1% also above 60000 counts. Deviations from linearity probably start very close to saturation only.

this case $\delta_t = +0.028$ sec. In both methods, data have been limited to exposure times shorter than 70 sec, i.e., intensity lower than $\simeq 50000$ ADU, to avoid significant strong deviation from linearity.

The analysis of the 2-D shutter effect on the MARCONI CCD produced results very similar to the ones obtained for the SITE1 CCD (Section 9.1.1). We applied the method described in Section 2.3 on data obtained on July 17, 2010 with LaRuca@1.5m equipped with the Marconi CCD (run V-020). The results are shown in Fig. 53. We notice that the MARCONI CCD is equipped with a 6 blade iris shutter while the previous one, the SITE1, was equipped with a 5 blade iris shutter. The performances of the two shutters are similar: the minimum exposure time to get a homogeneous illumination of the CCD is again $t \simeq 5$ sec.

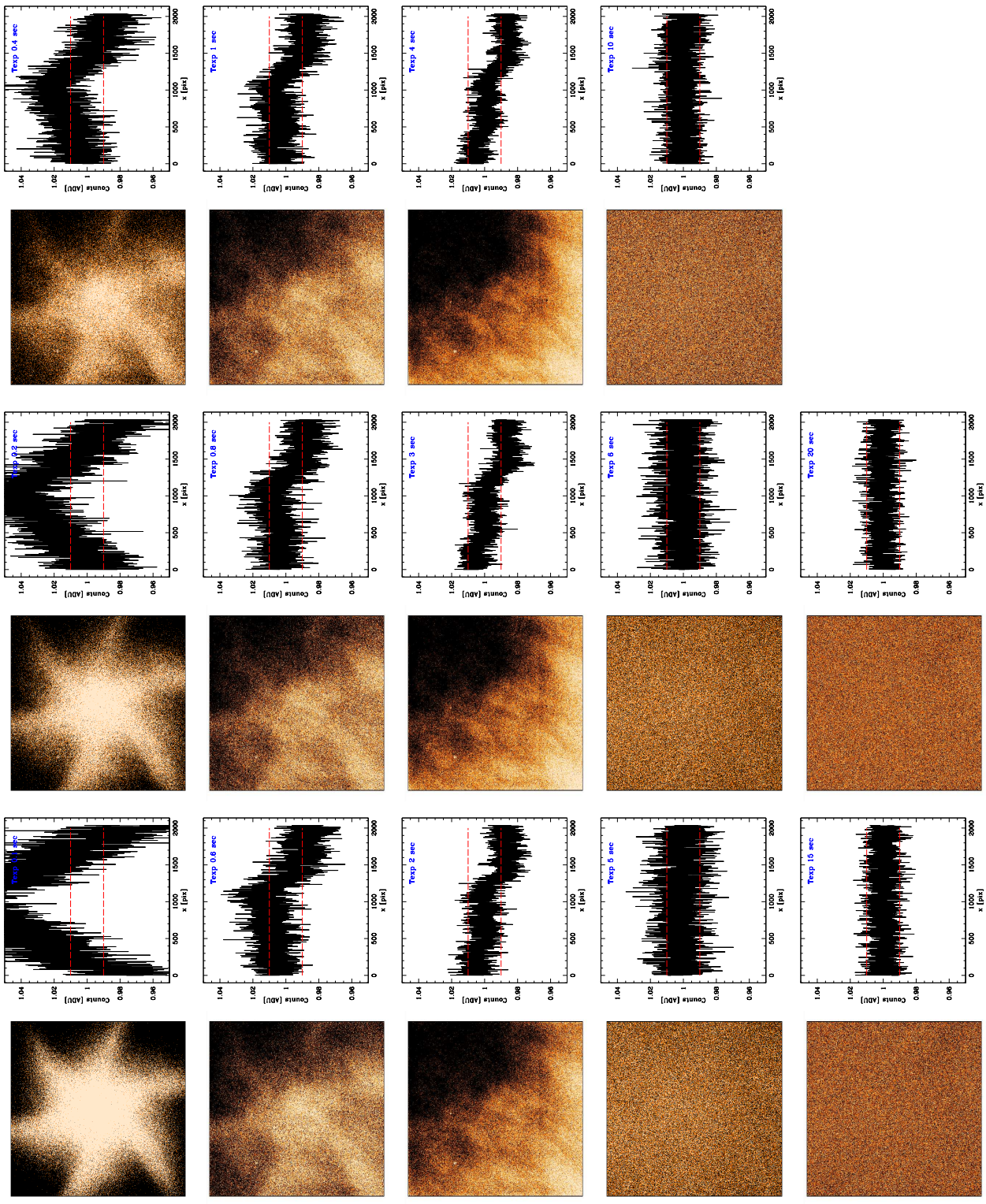

FIGURE 53: MARCONI CCD - Normalized ratio between masterflats with exposure time, from left to right, from the top to the bottom, equal to 0.1, 0.2, 0.4, 0.6, 0.8, 1.0, 2.0, 3.0, 4.0, 5.0, 6.0, 10.0, 15.0, 20.0 sec and to the 30 sec exposure. time masterflat. Colour cuts are the same for all images (z1=0.99 z2=1.01). The trace of the central row is shown on the right of each 2-D image. Data taken on July 17, 2010.

9.2 LaRuca CCD linearity

Our aim is to check the linearity of the response of the SITE1 Photometrics CCD (1072×1024 pixels) and of the Marconi e2vm E2V-4240 CCD (2154×2048pix.)[20] mounted on LaRuca@1.5m. Because LaRuca has no spectroscopic capabilities, we checked the detector linearity with the classic method (see Section 3.1).

9.2.1 SITE1 CCD - Linearity

The analysis of the SITE1 linearity is based on the same data acquired for the shutter test, already shown in Section 9.1.1 Fig. 54 shows that the SITE1 CCD is quite linear (within 1%) up to saturation. This results is confirmed also by Fig. 46 which shows that the CCD is linear within 1% also above 60000 counts. Deviations from linearity probably start very close to saturation only.

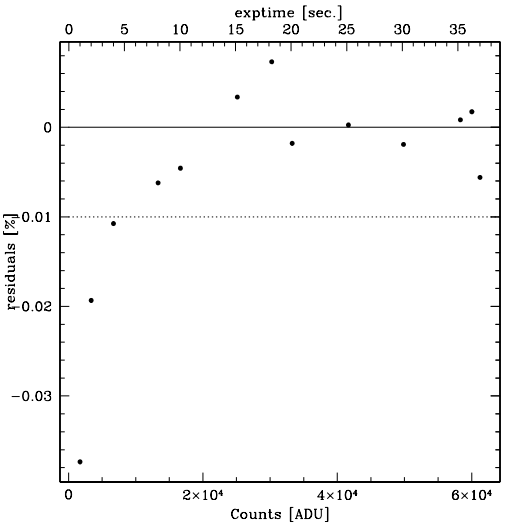

FIGURE 54: SITE1 - Deviation from linearity (i.e., residuals from the linear fit) of the CCD SITE1 Photometrics measured with photometric flat fields. At low counts (and short exposure times) the large residuals are due to shutter delay effects.

9.2.2 MARCONI CCD - Linearity

The analysis of the SITE1 linearity is based on the same data acquired for the shutter test, already shown in Section 9.1.2 Fig. 55 shows that the Marconi CCD is quite linear (within 1%) up to saturation. This results is confirmed also by Fig. 52 that shows that the CCD linearity is very good, with deviations smaller than 1% also above 60000 counts, probably increasing only very close to saturation.

[20] the SITE1 was the CCD in use before October 2009, when it was replaced by the new Marconi CCD.

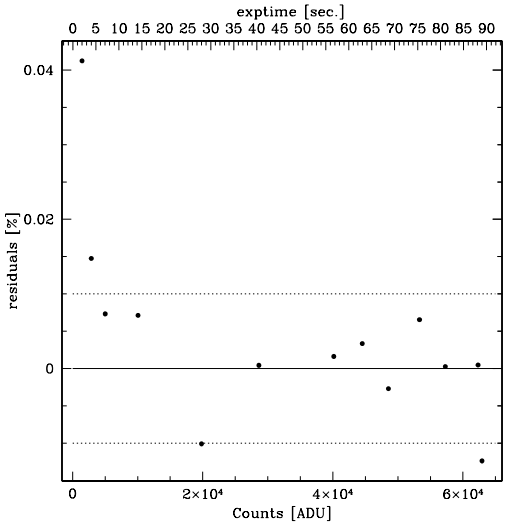

FIGURE 55: MARCONI CCD - Deviation from linearity (i.e. residual from the linear fit) of the CCD Marconi measured with photometric flat fields. The large residuals at low counts (and short exposure times) are due to shutter delay effects.

9.3 LaRuca Conclusions

The tests on the shutter delay and on the detector illumination do not depends on the detector, also because the physical size of the SITE1 and Marconi CCD are similar. The results suggest to avoid exposure times shorter than $\simeq 5$ sec if a homogeneous illumination of the whole frame is needed (more than 5 sec are recommended for absolute photometry). To be noted that relatively long exposure times are recommended non only for the scientific frames, but also for flat field frames. The shutter delay $\delta_t = 0.028 \pm 0.04$ sec (based on the most reliable values we obtained) must be added to the nominal exposure time. A 1 sec exposure corresponds to an exposure time $\sim 3\%$ longer, this effect can be neglected for longer exposure times, it is a 1% effect for a 3 sec frame, but the correction cannot, in any case, solve the inhomogeneous detector illumination.

The tests show that the CCD SITE1 Photometrics (used until October 2009) and the current Marconi e2vm E2V-4240 CCD are characterized by a good linear response (within $\sim 1\%$) up to $\simeq 60000$ ADU, i.e., close to saturation.

10 Conclusions

We summarize in Table 12 the results obtained for the instrument/detector analyzed in this document and listed in Table 2.
The shutter delay is negligible in relatively long exposure times, except for the old BFOSC shutter ($\delta_t \simeq -0.3$ sec). The longest shutter delay ($\delta_t = +0.028$ sec, LaRuca) is 1% of the exposure time for a 3 sec exposure, hence it can be neglected for longer exposure times.
The minimum exposure time to get a homogeneous illumination of the CCD varies from negligible (EFOSC2, DOLoRes, CAFOS-new diaphragm) to $\simeq 5$ sec (BFOSC, LaRuca).
We notice that all CCDs have a linear response (deviation within 1%) up to at least 55000 ADU (EFOSC2, CAFOS), some of them up to 60000 ADU (BFOSC, DOLoRes, LaRuca).
The results we obtained are constraints to be considered when observing with a given instrument and when reducing the corresponding data. For this reason the present document is complementary to the observations protocols (EP-001, EP-003) and to the data reduction and quality control protocols related to our observational campaign (SMR-001, SMR-002, SMR-003, SMR-004).

TABLE 12: Linearity and shutter effects for the Telescope/Instruments used in the absolute calibration programme of the Gaia spectro-photometric data

Telescope Instrument	CCD	Deviation from linearity	Minimum acceptable exposure time [sec]	Shutter delay* [sec]	Section
Cassini 1.5m	EEV 1300×1340B (new)	$\leq 1\%$ up to 60000 ADU	$\simeq 5$	-0.30 ± 0.05 before Feb. 2010	4
BFOSC	EEV 1300×1340B (old)	$\leq 1\%$ up to 55000 ADU		negligible afterwards	
ESO NTT 3.58m EFOSC2	CCD#40 LORAL/LESSER	$\leq 1.2\%$ up to $\simeq 55000$ ADU	< 0.1 if any	$+0.008 \pm 0.001$	5
TNG 3.58m DOLoRes	E2V4240 (new)	$\leq 1\%$ up to 60000 ADU	< 1 if any	-0.011 ± 0.002	6
CAHA 2.2m CAFOS	SITE#1d_15	$\leq 1\%$ up to $\simeq 55000$ ADU	$\simeq 3$ before Apr. 2008 < 0.5 after Sep. 2009	-0.017 ± 0.007	7
REM 0.6m ROSS	Marconi 47-10	n.a.	n.a.	n.a.	8
SPM 1.5m	SITE#1 Photometrics	$\leq 1\%$	$\simeq 5$	$+0.028 \pm 0.004$	9
LaRuca	Marconi e2vm E2V-4240	up to 60000 ADU			

* to be summed to the nominal exposure time

11 References

[GA-001], Altavilla, G., Bellazzini, M., Pancino, E., et al., 2007, *The Primary standards for the establishment of the GAIA Grid of SPSS. Selection criteria and a list of candidates.*, GAIA-C5-TN-OABO-GA-001, URL http://www.rssd.esa.int/llink/livelink/open/2736914

[GA-003], Altavilla, G., Bragaglia, A., Pancino, E., et al., 2010, *Secondary standards for the establishment of the Gaia Grid of SPSS. Selection criteria and a list of candidates.*, GAIA-C5-TN-OABO-GA-003, URL http://www.rssd.esa.int/llink/livelink/open/3033479

[GA-002], Altavilla, G., Federici, L., e Pancino, E., et al., 2010, *Absolute calibration of Gaia spectro-photometric data. III. Observing facilities for ground-based support*, GAIA-C5-TN-OABO-GA-002, URL http://www.rssd.esa.int/llink/livelink/open/3012989

Baldry, I.K., 1999, *Time-Series Spectroscopy of Pulsating Stars*, Univ. Sydney

[LF-001], Federici, L., Bragaglia, A., Diolaiti, E., et al., 2006, *Absolute calibration of Gaia photometric data. II. Observing facilities for ground-based support (pilot program)*, GAIA-C5-TN-OABO-LF-001, URL http://www.rssd.esa.int/llink/livelink/open/2706141

Leach, R.W., Schild, R.E., Gursky, H., et al., 1980, PASP, 92, 233, ADS Link

[SMR-001], Marinoni, S., et al., 2011, *Data Reduction Protocol for Ground Based Observations of SpectroPhotometric Standard Stars. I. Photometric Pre-reductions*, GAIA-C5-TN-OABO-SMR-001, Draft

[SMR-002], Marinoni, S., et al., 2011, *Instrument Familiarization Plan for ground based observations of SPSS. II. Calibration Frames Study and Reccommendations*, GAIA-C5-TN-OABO-SMR-002, DRAFT

[SMR-003], Marinoni, S., et al., 2011, *Data Reduction Protocol for Ground Based Observations of SpectroPhotometric Standard Stars. III. Quality Control on SPSS Photometric Frames and Photometric Catalogues Production*, GAIA-C5-TN-OABO-SMR-003, Draft

[SMR-004], Marinoni, S., et al., 2011, *Data Reduction Protocol for Ground Based Observations of SpectroPhotometric Standard Stars. IV. Short Variability Monitoring: Light Curves production and analysis*,

GAIA-C5-TN-OABO-SMR-004,
Draft

[PMN-003], Montegriffo, P., Bellazzini, M., 2009, *A model for the absolute photometric calibration of Gaia BP and RP spectra. III. A full in-flight calibration of the Model Parameters.*, GAIA-C5-TN-OABO-PMN-003,
URL http://www.rssd.esa.int/llink/livelink/open/2940357

[EP-001], Pancino, E., Altavilla, G., Bellazzini, M., et al., 2008, *Protocol for Ground Based Observations of SpectroPhotometric Standard Stars. I. Instrument Familiarization Tests*, GAIA-C5-TN-OABO-EP-001,
URL http://www.rssd.esa.int/llink/livelink/open/2858529

[EP-003], Pancino, E., Altavilla, G., Carrasco, J.M., et al., 2009, *Protocol for Ground Based Observations of SpectroPhotometric Standard Stars. II. Variability Searches and Absolute Photometry Campaigns Photometry Campaigns*, GAIA-C5-TN-OABO-EP-003,
URL http://www.rssd.esa.int/llink/livelink/open/2908205

Stello, D., Arentoft, T., Bedding, T.R., et al., 2006, MNRAS, 373, 1141, ADS Link